Calibration Report of the **STAFF** Measurements in the Cluster Science Archive (CSA)

Prepared by

P. Robert, C. Burlaud and M. Maksimovic

Version 3.0
Updated by N. Cornilleau-Wehrlin, P. Robert and R. Piberne

Version 4.0
Updated By R. Piberne and P. Robert

Version 4.1
Updated By N. Cornilleau-Wehrlin, P. Canu and R. Piberne

Version 4.2
Updated By N. Cornilleau-Wehrlin, P. Canu, R. Piberne and R.Katra.

Version 5.0
Updated By P. Canu, R. Piberne, R.Katra, V. Bouzid, C. Lacombe
And N. Cornilleau

Content

1. Introduction

The purpose of this document is to describe how the Cluster-STAFF data are calibrated, how these calibrated data compared with other Cluster instruments providing similar parameters and the limits of these methods.

In the first part, this document briefly describes the STAFF experiment, the calibration methods used, and the delivered products.

The second part presents a large number of cross-calibration studies, especially those with the DC magnetic field coming from the FGM experiment on Cluster, and summarizes the efforts done on this subject during the whole mission. The measurements by two common STAFF-SC and STAFF-SA frequency bands are also compared.

The cross-calibration results presented here are based on the presentations and discussions given between the first cross-calibration workshop in ESTEC in February 2006 and the final 24th CAA Cross-Calibration meeting held in Maspalomas Gran Canaria, 26-28 November 2018.

Most of the studies presented here are developed in the article **CLUSTER STAFF search coils magnetometer calibration – comparisons with FGM** [12].

A number of authors have been involved in this work, including P. Robert, N. Cornilleau-Wehrlin, C. Burlaud, M. Maksimovic, L. Mirioni, V. Bouzid, R. Piberne, P. Canu, Y. De Conchy, C. Lacombe, B. Grison, O. Santolik, O. Alexandrova and D. Attié.

Remark: The previous versions of this Calibration Report present earlier stages of the methods used up to 2012 to calibrated the STAFF-SC waveform data, which were not archived. The first comparisons with respect to FGM data show significant underestimation of the STAFF-SC measurements which have been understood and corrected. The origin of these underestimations and the corrections applied to the final products are described in [12].
This last version of the report is limited to the description of the final methods used to calibrate all the STAFF-SC products present in the final archive.

2. Instrument Description

The CLUSTER STAFF experiment comprises a tri-axial search coils magnetic sensor (0.1 Hz – 4 kHz frequency range) and two on-board wave analyzers, a magnetic waveform unit (STAFF-SC) and a wave spectrum analyzer (STAFF-SA) that calculates the complete matrix for the 3xB + 2xE components. The electric waveform data are received from the EFW sensors. For more details on the experiment, see references [1][2]. For information on the coordinate systems used, see Appendix A: Coordinate systems used by STAFF

Note: In this document, general convention for science data set the spin axis in Z direction.

2.1 STAFF-SC

- The magnetic waveform unit delivers 3 waveforms (B_x, B_y, B_z) from the pre-amplifier filtered in one of the two low-pass bandwidths, 0.1 - 10 Hz (Normal Bit Rate: NBR) and 0.1 - 180 Hz (High Bit Rate: HBR). Sampling rates are 25 and 450 Hz, respectively.

- The filtered signals are digitized by three 16-bit sampling-and-hold devices, synchronized by DWP and sent to the DWP experiment.

- The A/D converters are the same for STAFF and EFW and synchronized by DWP in order to facilitate further combined wave analysis. The low pass filters are identical.

- Due to the telemetry limitation, a compression from 16 to 12 bits is performed inside DWP for STAFF wave form data.

- The coordinate system of the Raw telemetry data is the Sensor Coordinate System (SCS), as described in Appendix A: Coordinate systems used by STAFF ; this is a spinning frame, where Y and Z axis are perpendicular to the spin axis and X is parallel to the spacecraft spin axis.

- **NOTE**: In order to comply with other instrument reference frames, the X and Z axis are exchanged and processed in the Data Sensor System (DSS) where Z is along the spin axis, for producing the archived non-calibrated L1 (DWF) data and for the calibration of raw Waveform STAFF-SC to Level 2 – (CWF) data.

- Level 2 calibrated waveforms (CWF) are produced in the GSE and in ISR2 frames.

- Level 2 calibrated complex spectra (CS) are produced in the GSE frame.

2.2 STAFF–SA

- The spectrum analyzer is designed to calculate the complete cross-spectral matrix for the 5 available components, 3xB + 2xE, in the 8 Hz-4 kHz frequency range. The electric field components come from the EFW sensors.

- The analysis band is divided into 3 logarithmically distributed frequency sub-bands of 9 frequencies each.

- For each sub-band there are 3 automatic gain control (AGC): one for Bz channel (parallel to the spacecraft spin axis) and one for each couple of spinning components (B_x, B_y and E_x, E_y respectively).

- The different modes depend on the combination of 3 parameters: the time resolution, the number of frequencies computed (2 or 3 bands) and the number of wave components considered.

- Products are delivered in the ISR2 coordinate system (inverse of SR2, close to GSE).

3. Measurement Calibration Procedures

3.1 Calibrations procedures

This term overlaps different aspects:

- The calibration methods used to transform L1 data (waveform or spectra) into level 2 (L2) calibrated data.

- The corresponding software, that take for input L1 data files and calibration files, and produce L2 data files.

  The calibration files consider the whole transfer function, including the sensors, the pre-amplifiers and eventually the filters. These files can be regularly updated by the exploitation of calibrated signals recorded during the on-board calibration mode executed once per orbit and stored in the L1 data files. The use of these calibrated signals has allowed to verify that the STAFF experiment performances have not changed since the commissioning phase. ***The final calibrations files used to calibrate the waveforms have been consolidated in 2011 and used to deliver all calibrated waveforms (CWF) and spectra (CS) during the whole mission from commissioning to end of life data in 2024***.

3.2 Cross–calibration procedures

In order to check the validity of the STAFF calibrated products, some comparisons can be performed within STAFF products and with calibrated products coming from other instruments. There are several possibilities for these cross-calibration activities:

- The STAFF-SC NBR mode delivers magnetic waveforms up to 10 Hz. So, comparison with FGM data can be done at three levels:

  - The Doppler effect due to the STAFF sensor rotation into the DC magnetic field provides a strong sine signal in the spin plane. On this strong sine signal are superimposed the very low amplitude magnetic fluctuations. Once the sine signal is extracted, its amplitude and phase are determined and corrected by the

transfer function. These X and Y calibrated components of the DC magnetic field in the spin plane can be directly compared with FGM data.
  - The 3 STAFF-SC calibrated waveforms, from about spin frequency (0.25 Hz) up to 10 Hz, can be compared to the FGM high-resolution waveforms in any coordinate system.
  - To check a possible dependency with frequency, the corresponding spectra can be also compared. This provides additional information on each instrument, sensitivity versus frequency.

- The STAFF-SC HBR mode delivers magnetic waveform up to 180 Hz, and so permits an overlap with the low part of the STAFF-SA frequency range (usually 64 Hz - 4 kHz in HBR, but some dedicated mode may allow a comparison from 8 Hz). Thus, the spectra level and the spectra continuity of the two sub-experiments can be checked.

- For STAFF-SA, in addition to the cross-calibration mentioned above, it is possible to check the spectral continuity of the fields fluctuations with other Cluster instruments:

  - WBD (between 25 Hz and 4 kHz)
  - The spectral continuity of the electric fluctuations with EFW in the same conditions as for the magnetic components as described above for STAFF-SC and STAFF-SA
  - WHISPER (between 2 kHz and 4 kHz)

4. Calibration Processing Procedures

The two components of STAFF, SC and SA provide data through very different analysis. The waveform for SC requires significant computer processing on the ground for getting the calibrated data from samples received in the telemetry stream. Spectra and Cross components values are calculated on board for SA, for which most of the calibration information was obtained on ground prior to launch. Some information on the processes used for these calibrations are listed here.

4.1 Cleaning STAFF-SC waveform procedures

As explained in 3.2, the Doppler effect due to the STAFF sensor rotation into the DC magnetic field provides a strong sine signal on the components perpendicular to the spin axis (X and Y). This sine amplitude is equal to the perpendicular DC magnetic field (from a few nT up to ~1200 nT, value above which the STAFF signal saturates). On this strong sine signal are superimposed the very low amplitude magnetic fluctuations (~a few nT or less).

First, before the FFT procedure, it is necessary to remove this strong sine signal. Then, the FFT will be applied on the remaining useful signal. This process consists of fitting the signal with a pure sine signal, whose frequency is known (the spin frequency). The dedicated process, based on a harmonic analysis applied on a single spectral component, provides the fitted sine signal amplitude and phase. Note that those two parameters are useful for FGM DC field

comparison. Finally, this pure sine signal is subtracted from the original one to retrieve the fluctuations. This process is very efficient in terms of rejection performance and CPU time. But it requires at least a minimum duration of two spin periods, where the DC field is supposed to be constant. For long-time windows, only a DC field average value is subtracted, and so the efficiency of the rejection is decreased. In any case, all frequencies are preserved, but the spin frequency. As we can see, one has to choose the best compromise between a not-too-short and a not-too-long window duration.

4.2 Classical calibration method for STAFF–SC

This method operates in up to 5 steps depending on the desired final product and is the base used to produce calibrated spectra (CS).
These steps are:

4.2.1 Get Level 1 waveform transformed from TM counts to Volts as a series of successive windows.

→ *Selecting window time length (Δt) determines the frequency resolution (Δf) as Δt.Δf=1.*
→ *TM count [0-65535] to Volt [-5V, +5 V].*

—►Calibration step # **1**: Volts, Data Sensor system (DSS), with DC field.

4.2.2 "Cleaning" raw waveforms in the spinning Data Sensor System (DSS).

→ *Remove the in tone signal (~ 1 nT up to ~ 2000 nT) high compared to the useful signal (~1 nT or less). This is done using a specific harmonic analysis process. There are then 2 data sets, waveform in TM volts without DC components and DC components XY kept for further use. Those XY spin plane components are calibrated for step 5 processing and future FGM comparisons.*

—►Calibration step # **2**: Volts, DSS without DC field.

4.2.3 Calibration of each component in a given window.

→ *Signal Centering, trapezoidal windowing, FFT, complex transfer function including conversion from Volt to nT, correction by *1/G(f),*

➔ *At this step one gets the complex calibrated spectra in the Data Sensor System*
➔ *To go back to time domain: cutoff at low frequency*
- *0.1 Hz for further transformation into SR2/ISR2 reference frame,*
- *0.6 Hz for further transformation into GSE.*

Then apply an FFT^{-1}.

—►Calibration step # **3**: nT, DSS without DC field.

4.2.4 Get calibrated time series data in nT, in a fixed reference frame.

→ *Apply the appropriate matrix, but it requires accurate spin phase computation from the Sun pulse.*
→ depending on the desired reference frame, use the data set produced after either one of the filtering (see above)

—►Calibration step # **4**: nT, fixed SR2 system, without DC field,

the reference frame can be changed to other system, like GSE used to produce Calibrated Spectra (CS).

4.2.5 Add DC field values on X and Y

—►Calibration step # **5**: nT, fixed SR2 system, with previous calibrated X-Y DC field.
This processing allows comparing STAFF and FGM spin plane components data.

The DC field is not added on the Z axis since it is very weak and not significant, due to the very low difference between the Z and spin axis (less than 0.5°).

Note that if this method is well adapted to compute calibrated spectra, it does not allow getting a continuous calibrated waveform, because the edges of calibration window are disturbed by the weighting function. The continuous calibration method has thus been developed, tested on significant data and applied to produce the full CWF data sets (see 4.3). Various tests have been done to check the validity of this method with respect to the classical one.

4.3 Cluster STAFF-SC Continuous calibration method for CWF

The continuous calibration method is based on the classical method. Data are processed as a series of successive windows but now spaced by one or a few TM samples (at 25 or 450 Hz), that implies an overlapping of 2 successive windows. Then a Gaussian windowing is applied, and only the central point (or a few central points), corresponding to the Gaussian maximum, are kept. The next window is taken by a time shift of only one (or a few) TM sample.

The diagram hereafter summarizes this method:

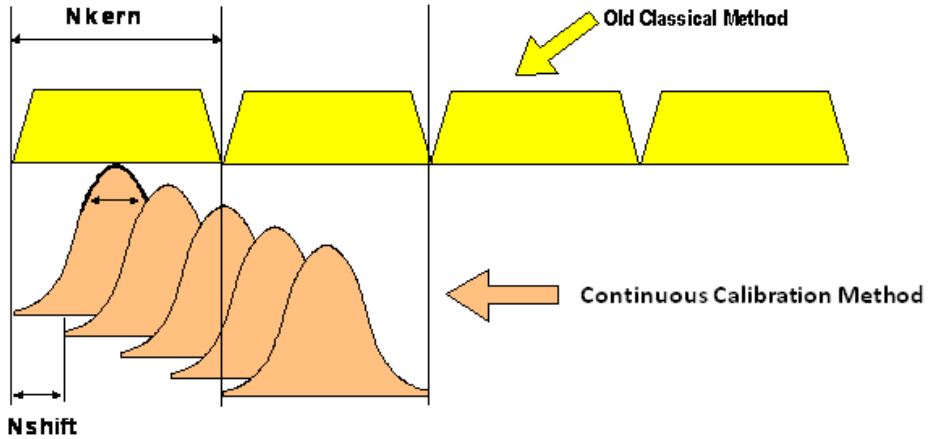

Figure 1: The schematic drawing of the two methods used for the production of continuous waveforms.

This method avoids getting discontinuity on each window edge and a continuous calibrated waveform is also obtained. However, it requires much CPU time.

Nkern must be chosen to - do a correct despin (> 2Ts, but not too long, ex: 512 points)
- have a high enough frequency resolution (not too short)

Nshift: - can be as short as possible (ex: 2 pts)
- could be extended to reduce CPU time without damage for the calibration quality (could be 6-8 pts)

The parameters chosen for the CWF datasets (GSE & ISR2) delivered to the CSA are:

Nkern = 1024 in NBR / 4096 in HBR and Nshift = 2.

These values were chosen as the best compromise for mass production, to see the maximum of events. This also implies that, for specific events, the calibration of data can be improved with specific Nkern and Nshift values.

Note 1: In a first approach, the classical method has already been improved by a more efficient despin, (and so a better calibration), which is used in the continuous method. In particular, the phase continuity of the spin signal has been imposed.

Note 2: This method, working in the frequency domain, is comparable to the one chosen for the SCM data of the NASA-Themis mission, where the calibration process remains in the time domain, and perform a convolution between the signal and the inverse of the impulse response of the transfer function. This is the same thing in term of mathematical approach, but different in term of coding. The choice of the frequency domain allows a more straightforward coding, and benefits from pieces of code already existing.

4.4 STAFF-SA Calibration Procedures

The STAFF Spectrum Analyzer is a fairly complex instrument based on the on-board computation of spectra after collection of the required samples. It is based on 3 frequency bands of 9 steps each, with 3 AGC (one for each plane components, Bx&By, Ex&Ey, one of Bz) with 256 possible values. The large numbers of values for a complete calibration of each of the SA instrument on the 4 spacecraft leads to simplify the on-ground calibrations and to limit the testing/calibration on only some of these values. It was assumed that the 7th step of each frequency band and the step 80 of each AGC were correct and were used to build the transfer function. This hypothesis was not fully verified in flight and introduce some incorrect values to the frequencies 70 Hz, 140 Hz and 280 Hz, which appeared as interference lines on the spectrograms (for further details see [12]). Correcting these anomalies after their identification might have been possible, but qualified personnel for this work were no longer available, so no further action was taken. There are also some limits in the quality of inter calibration between each of the frequency bands. Details are presented in §5.2.

4.5 Full processing line

The logical flow diagram hereafter describes the full processing from raw data to level3 (L3) products.

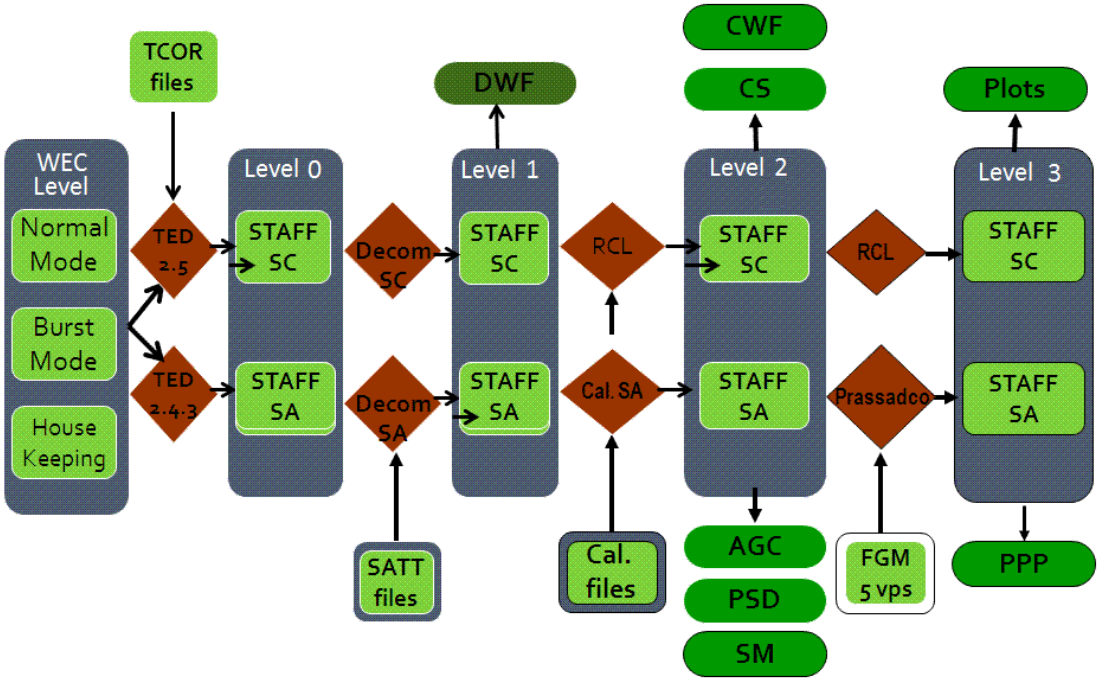

Figure 2: Processing chain for the data production.
The data products in green are delivered to the CSA.

Remarks:

- The TED (Telemetry Extraction and Decommutation provided by the DWP team) software version used to timestamp the data is different for STAFF-SC and STAFF-SA. For details, see UG or ICD.

- The STAFF-SC L1 data files, also called Decommutated Waveforms (DWF) are delivered to CSA because it is the only data pack containing all initial data (information about block data format, timestamps, compression quality, etc.), before any transformation such as calibration or change of reference frame.

- STAFF-SA calibration is done by dedicated software [7].

- STAFF-SC calibration is done using a part of RCL software. RCL (Roproc Command Language) is a set of commands allowing many different data processes on time series data from spatial experiments. This is an overlay of the Roproc software (P. Robert's procedures). RCL software allow the processing of CLUSTER data as well as waveform

data from any project/experiment, on many platforms and Operating Systems (tested on SUN/Solaris, Linux, Windows).

- The L2 to L3 processing is done by RCL for STAFF-SC and PRASSADCO for STAFF-SA (see [8]).

5. Result of calibration activities

5.1 Consequences in CWF/CS of multiple irregular data gaps

The calibration methods used for CWF and CS (described above) rely on continuous time series of digital waveform (DWF). During periods of poor spacecraft telemetry (hatched telemetry) and then discontinuous time series, there will be missing CWF and CS which will extend beyond the period of the missing samples. This will induce missing data periods, different between these 2 datasets because of the different calibration methods and parameters used.

As explained above, CWF are calibrated using "continuous calibration" while CS are calibrated with the "classical" calibration method (contiguous windows). The parameters that were chosen as a compromise to obtain the maximum of events is the following:

- For CWF:
  - NBR default window: 1024 pts
  - HBR default window: 4096 pts

  Calibration window shift = 2 points (default).

- For CS:
  - NBR default window: 256 pts
  - HBR default window: 4096 pts

  The window is entirely shifted.

We see that the parameters are not the same in NBR mode. This non-homogeneous situation may lead to produce CS and not CWF when the telemetry is hatched, depending on the time delay between missing samples.
Indeed, in NBR mode, **if one point is missing in DWF**, this will result in the 511 previous and 511 next points not being calibrated, while only the current window of 256 points not being calibrated in CS. So, if we have consecutive windows of 1024 points with only one point missing in each of these windows, **there will be no CWF data produced at all while CS data will contain 2 to 3 calibrated spectra in each of these windows.**

An example is plotted below in Figure 3:

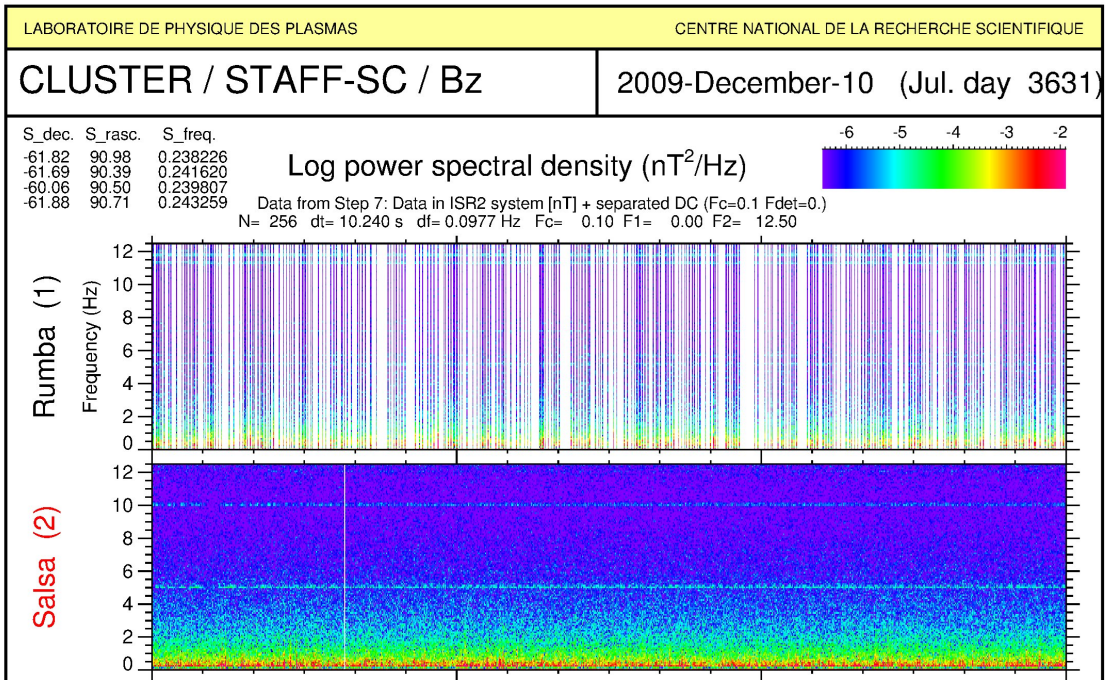

Figure 3: Example of CS data obtained with hatched telemetry in NBR mode for C1

We can see that despite the numerous missing spectra, the PSD seen by C1 is pretty similar to the PSD seen by C2. But for this day, no CWF are produced for C1.

We can note that such cases will only appear in NBR mode, due to the in-homogenous choice of the calibration window (1024 for CWF versus 256 for CS).

Figure 4 and Figure 5 show the different impact of non-continuous time series the same day in NBR and HBR mode while C3 telemetry was hatched for long periods of time.

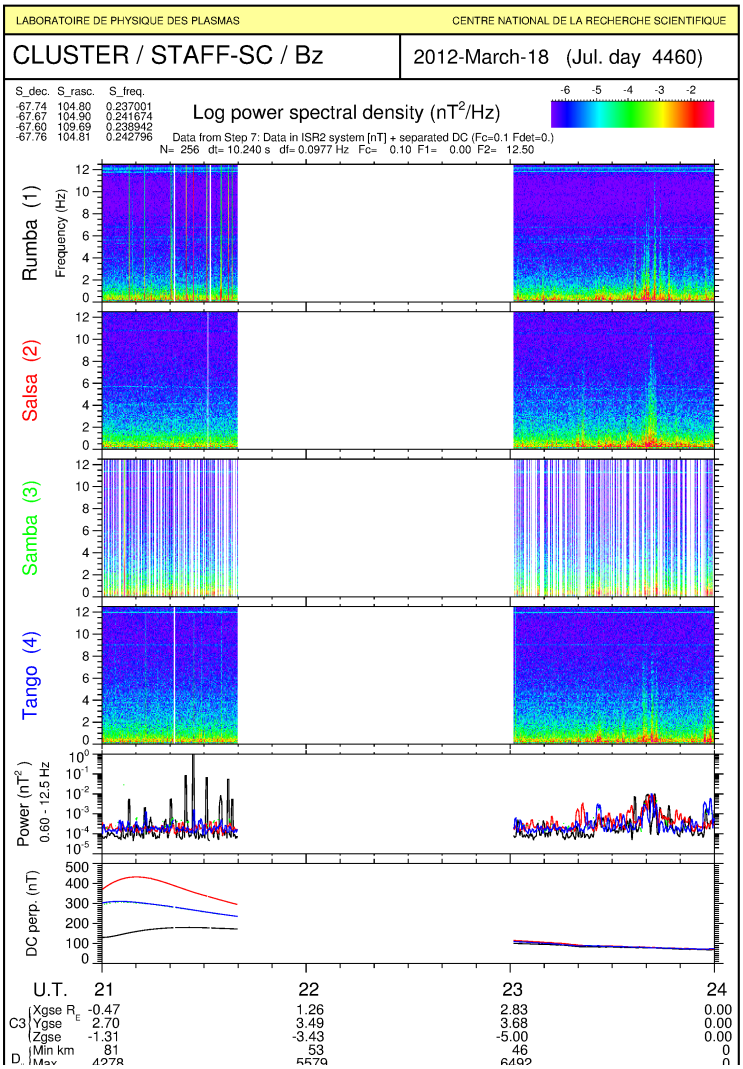

Figure 4: 2nd example of CS data obtained with hatched telemetry in NBR mode

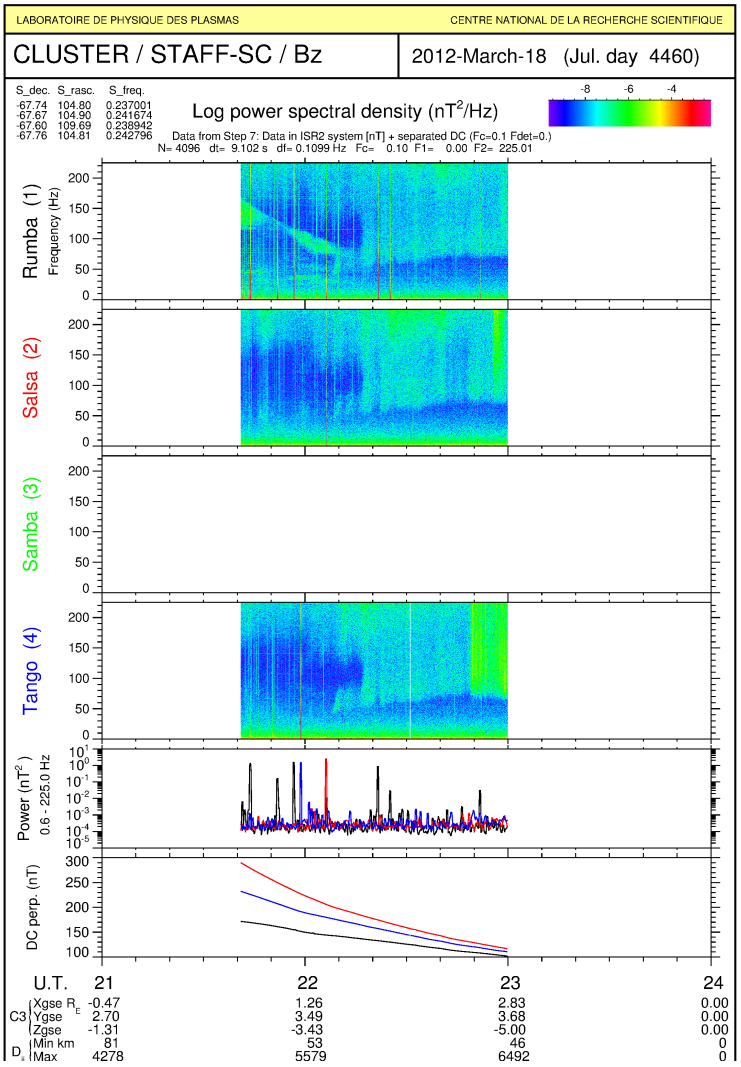

Figure 5: Example of CS data obtained with hatched telemetry in HBR mode

As expected, there is some data only in NBR mode and not in HBR mode.

5.2 Limits in the SA calibration

5.2.1 Interferences lines

The complexity of the Spectrum Analyzer calibration leads to rely on few calibration parameters. The 7th step in each A, B, C frequency band and the AGC = 80 (among 256) value, were considered as correct, to build the transfer function that converts raw telemetry data into calibrated values. This assumption was not confirmed by data collected in-flight and induce some overestimated values which appear as horizontal lines on the dynamic spectrograms. Figure 6, (Electric at left and magnetic at right) shows how these lines appear on the 4 S/C as interference during a quiet period. The signature of these interferences is different between spacecraft and between electric and magnetic and their level can

significantly be modified by the observed waves, depending on the power and frequency. The interference lines are always more visible on C3. There is also a small interference line, seen ~900 Hz in Band C which is internal to WEC and is due to DWP. No solution was found to resolve these calibration issues, identified after some years of operation. This would have required considerable effort, and the team responsible for this ground calibration was no longer available.

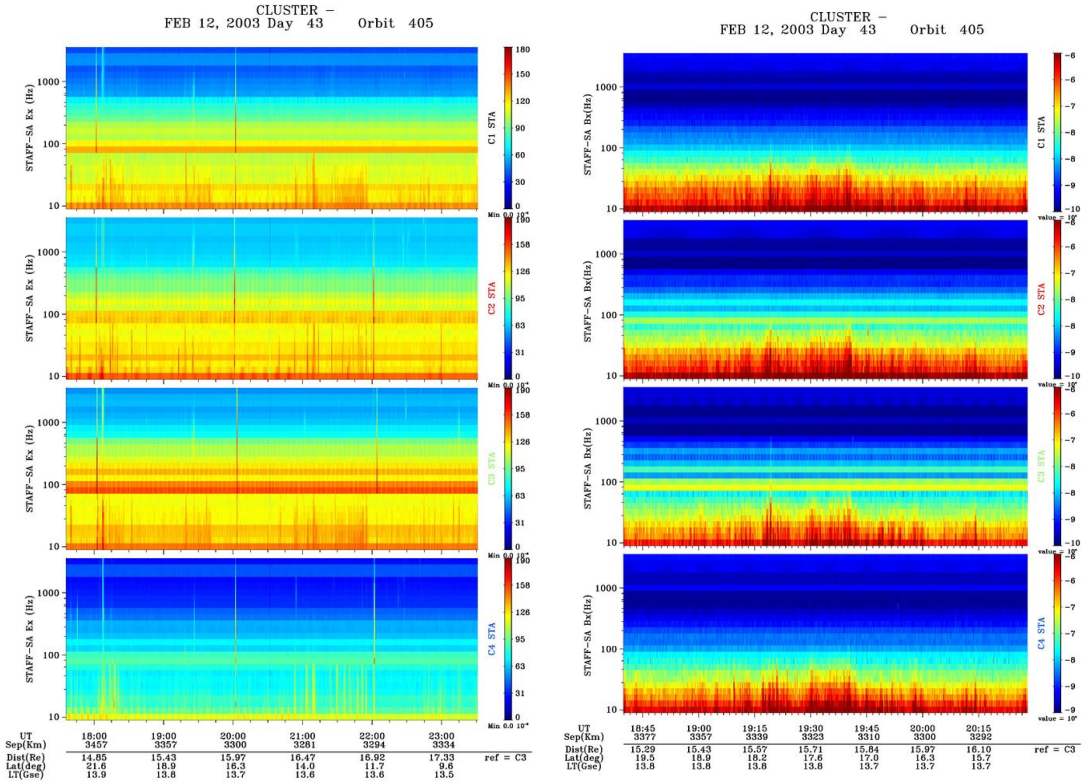

Figure 6: Interferences (E left, B right) due to ground calibration limits observed on the 4 SC

5.2.2 Intercalibration between frequency bands

Sudden discontinuities can be observed in some spectra at the edge of the A, B, C frequency bands. This may also induce corresponding sudden changes in polarization parameters calculated from the cross-spectral matrix. Figure 7 below shows such discontinuities appearing, both in electric (top) and magnetic components (bottom), between band A and B (~70 Hz) and B and C (~500 Hz).

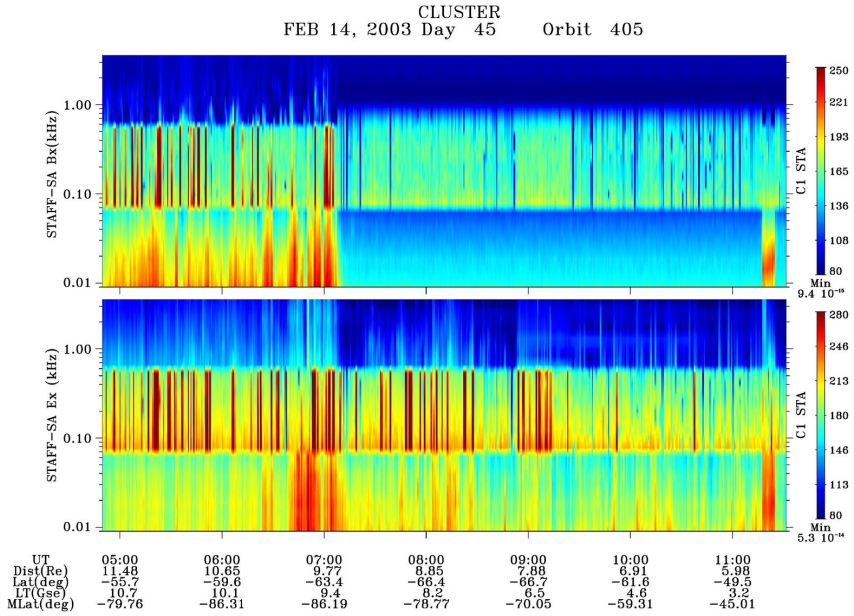

Figure 7: Discontinuity in spectra at edge of frequency bands

These anomalies could be explained by the characteristics of the Spectrum Analyser and its limits in responding to very impulsive emissions, the AGC and the Despin system having possible impacts on the spectra.

5.2.2.1 AGC impact

There are 9 AGC in total, 3 AGC on each of the 3 Frequency bands: one for each of the spin plane sensors (BxBy, ExEy) and one for the spin axis magnetic sensor Bz. The spin plane has common AGC to avoid a modulation of the signal induced by the spacecraft rotation.
The sampling frequencies and integration times for these AGC are:

	Sampling Frequency	Integration time
Band A (8-64 Hz)	250 Hz	960 ms
Band B (64-512 Hz)	2 kHz	120 ms
Band C (512-4000Hz)	16 kHz	15 ms

This corresponds, for each band and each sensor, to 256 samples, from which the DFT analysis derive 9 frequency steps. These values are then averaged on board to fit in the TM allocation, depending of the selected mode (usually 1s in NBR, 0.250 s in HBR)
Note that each AGC will probably not correctly represent signal bursts shorter than its integration time. Additionally, it will likely take a long time to recover from intense bursts, probably several 100 ms for the A band.
The SA instrument is particularly well suited to analyzing low-power signals with slow temporal variation, such as radio emissions. However, it is likely to be less effective in providing accurate spectra across all three frequency bands when dealing with strong, sporadic plasma emissions, such as those occasionally observed by Cluster. In these cases, electrical components are particularly affected by powerful, short-lived electrostatic bursts.

5.2.2.2 *Impact of Despin*

While the calculation of the despin for SCM (see 4) consists of removing the static magnetic component, the despin for SA aims to correct the amplitude of a signal, which can be directional and modulated by the rotation of the spacecraft. For each frequency the power is corrected from the averaged power of the frequency band modulated by the spin phase of the spacecraft. This is done for E&B components, for Band A and B. The modulation for Band C is negligible during the acquisition time. Here again, this correction makes sense for emissions presenting a low variation over time comparable to the spectrum acquisition time, but can have unfavorable results for bursts of short duration.

5.2.2.3 *Example of SA observation of short electric bursts*

This can be illustrated by the example below, where low, recurrent ESW bursty emissions were observed during the day. These emissions resulted in large frequency bands after spectral analysis. On Figure 8 below, which displays the Ex spectra on C1&C3, these signatures are observed with relatively low power, with the standard broadband, decreasing power with frequency spectra. No induced artifact between the 3 frequency bands is observed.

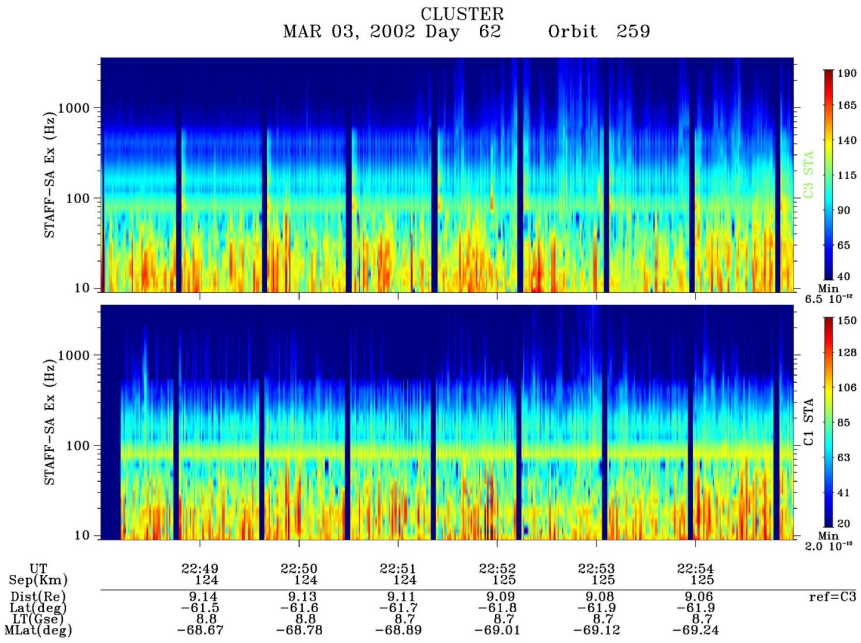

Figure 8: Observation of low power ESW on SA Electric Ex

The spectra are quite different a few hours before, when frequent, more powerful ESW bursts are detected on SA electric spectra (Figure 9 top). The spectra show obvious power changes at the edges of the frequency bands, where the discontinuity between bands A and B is most obvious. Figure 9 (bottom) zooms in on part of these observations, where the spectra and the onsets of the edge peaks are clearly visible.

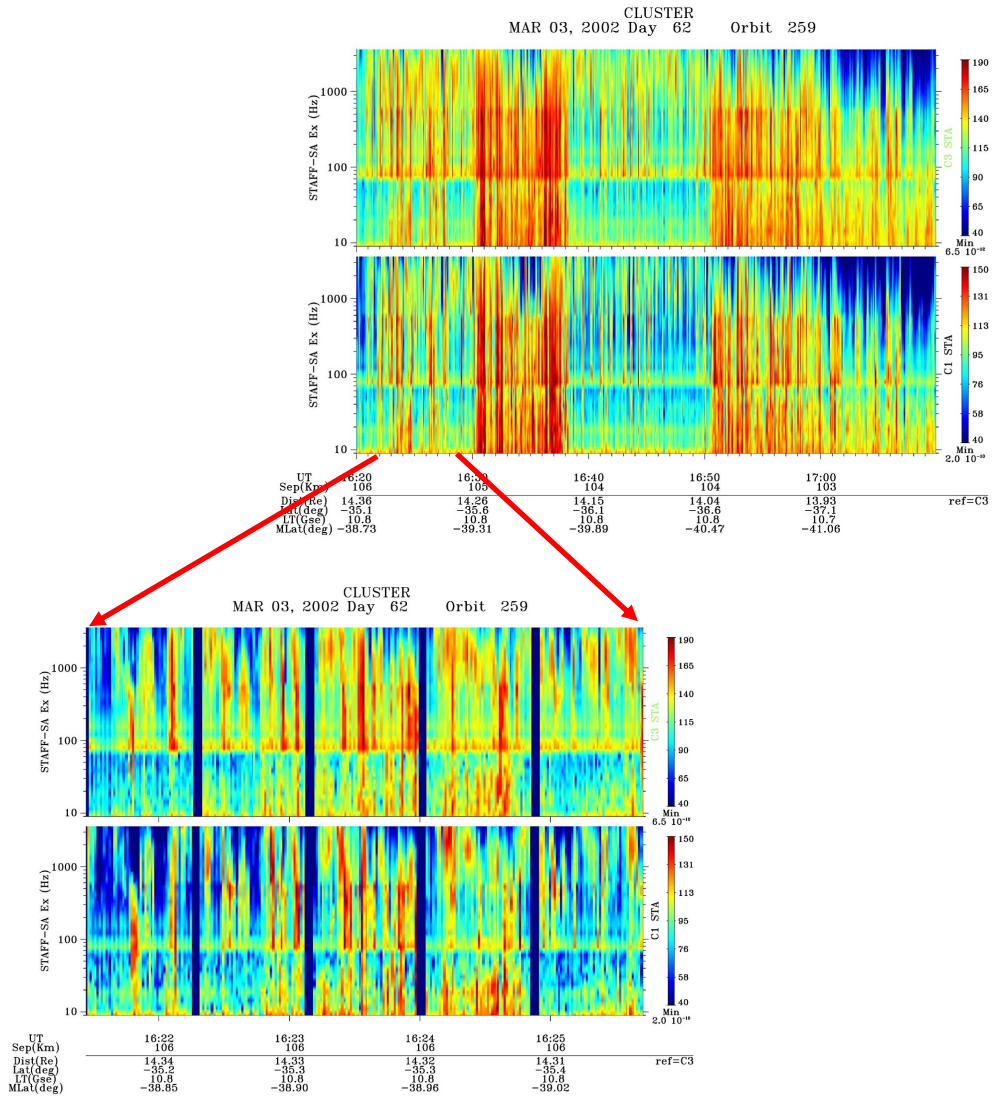

Figure 9: Discontinuities in Ex spectra for short duration burst of electrostatic emission Details is shown at the bottom

5.2.2.4 Conclusion and recommendations

Although the STAFF Spectrum Analyzer generally provides very good data with electromagnetic waves exhibiting small variations in time, power, and frequency, users should be cautious when short-duration bursts are observed. This can generate spectra with frequency discontinuities similar to those shown above. Since these signatures are highly depending on the emission duration, peak frequency and bandwidth, no systematic reconstruction of the calibration of archived spectra had been carried out. The users should carefully check the context of the observations before attempting such reconstruction.

6. In Flight Calibration

To check the quality of the magnetic measurements in flight and monitor its potential evolution over time, the in-flight calibration of the 3-axis search coils was systematically carried out, at least once per orbit (See the STAFF User Guide § 13.4 for the presentation).
The 23 steps of this operation, both for SCM and SA of a calibration sequence, are reported on STAFF Status Word number 1 and a full description of these steps is provided in Appendix B: In-Flight Calibration mode. The corresponding telemetry was processed like standard waveform and the produced spectra analyzed. A small text report was systematically produced for each in-flight calibration sequence. These reports have been archived at CSA. Their content is presented also in Appendix B: In-Flight Calibration mode. The most significant steps have been plotted for different periods of the mission. This allows to compare both the potential difference between the spacecraft and the evolution during the unexpected 24 years duration of the mission, compared to the 2 years of operations for which the instruments were built.
Similar analyses of the calibration sequences were performed for SA but not on a systematical basis. They are not archived at CSA.
The results are illustrated here by comparing these in-flight calibration spectra obtained during the mission and between the STAFF search coil instruments on each of the 4 Cluster.
The figures below displayed the spectra of the output obtained from the strongest white noise signal generated during the calibration sequence. The spectra, which can be assimilated to a trace of the transfer function of each search coil, is an averaged over steps 1-4 (see Appendix B: In-Flight Calibration mode). Step 23, which is the spectrum obtained without any generator stimuli, represents the background noise observed at the same time.
Users should keep in mind that the results of each step are only valid in absence of significant natural noise around the spacecraft and are representative on the search-coil response to the stimuli generated by the calibration box. Step 23 (no stimuli, generator off) provides values which can be compared to the instrument background noise and thus validates the calibration sequence. The calibration sequences plotted were obtained during quiet periods.
Figure 10 presents a superposition of the results obtained in NBR mode for the Bz axis between each spacecraft at the beginning (2001 left) and end (2024 right) of the mission. This shows that the good inter calibration between spacecraft, which was below 2% in amplitude during ground calibration tests, was also observed in-flight and has not changed at the end of the 24 years of the Cluster mission. Similar good results were obtained on Bx and By axis.

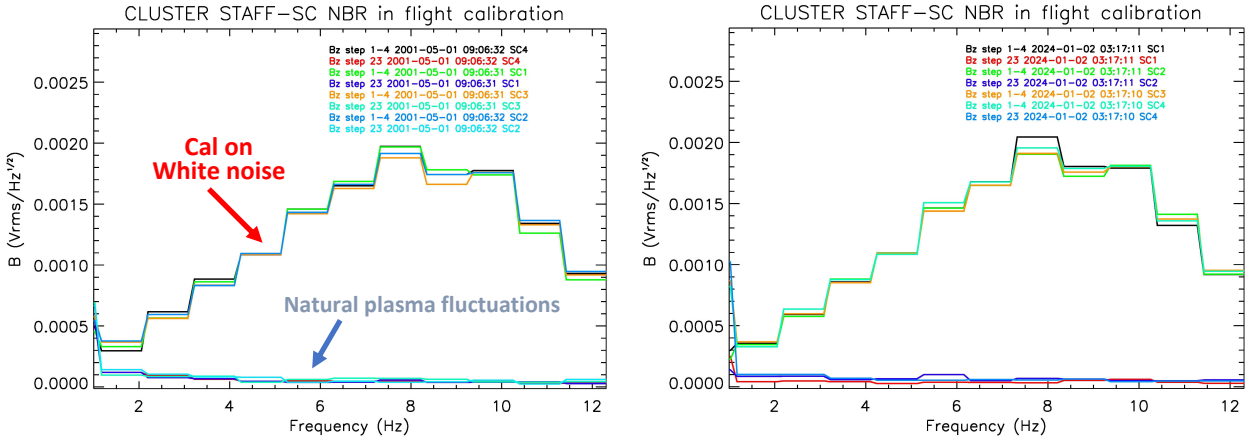

Figure10: Overlay of in-flight calibration results for four spacecraft in NM At the beginning of mission (2001 left) and end of mission (2024 right)

Figure 11 shows, with similar outputs, that these values had not changed at different steps of the mission, and was also verified between spacecrafts. Same constant calibration results were observed during HBR in-flight calibration (Figure 12).

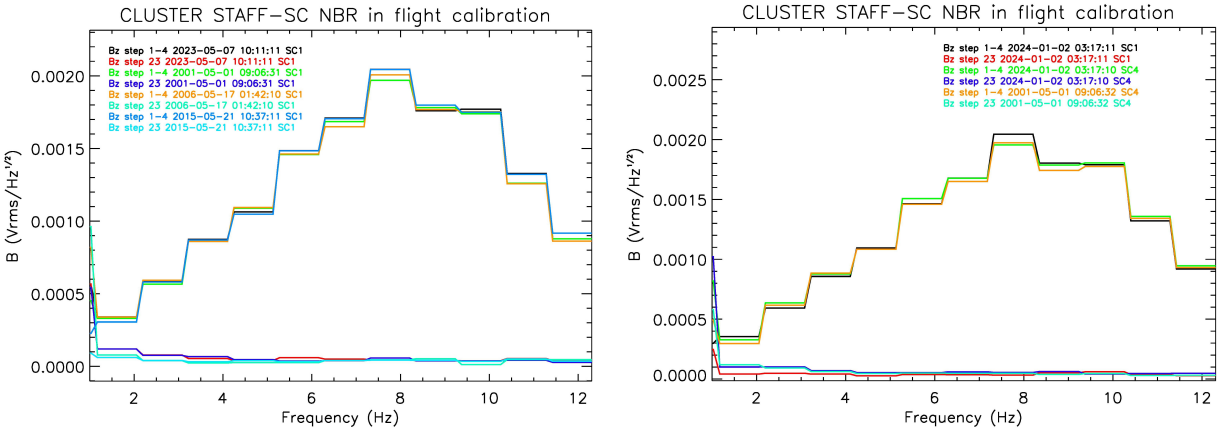

Figure 11: Overlay of in-flight calibration results between 2001 and 2023 in NBR for C1 (left) Overlay at beginning (2001) and end (2024) of mission for C1 and C4

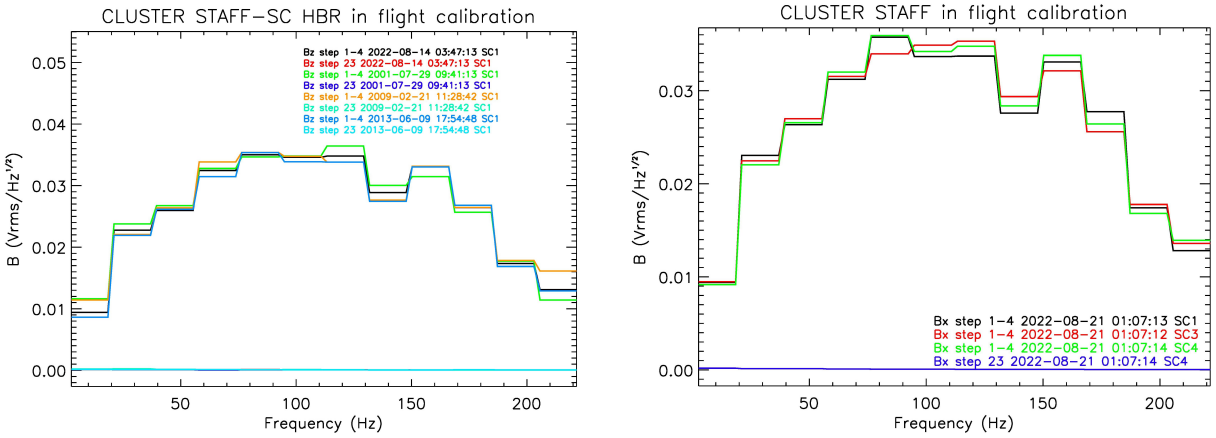

Figure 12: Overlay of in-flight calibration results in HBR between 2001 and 2022 (left) and between the 4 spacecraft in 2022(right)

Conclusion: The transfer function used to calibrate the STAFF measurements, which was essential in the combined analysis of data between spacecraft and necessary for the derivation of certain plasma parameters such as electrical currents, did not change significantly between spacecraft and during the entire mission.

7. Results of Cross-Calibration Activities

7.1 Comparison of measurements between STAFF Instruments

There are different ways to check the good quality of the observation with the archived calibrated data, internal to STAFF and by comparing STAFF data to other instruments.

7.1.1 Comparison of data obtained with short separation distance

Although direct comparison of STAFF observations obtained simultaneously by different satellites seems difficult due to the evolution of these emissions on a scale comparable to the spacecraft separation expected during the nominal mission, there are a few examples during the mission extension where the separation distance between two spacecraft was small enough to expect similar plasma conditions.
Figure 13 below shows the direct comparison of the waveforms (CWF) obtained in 2015 by C3 and C4 during a period where the spacecraft were separated by ~6 km. The waveforms, here in the most challenging BM mode for this comparison, are almost identical, confirming the excellent calibration of the instruments.

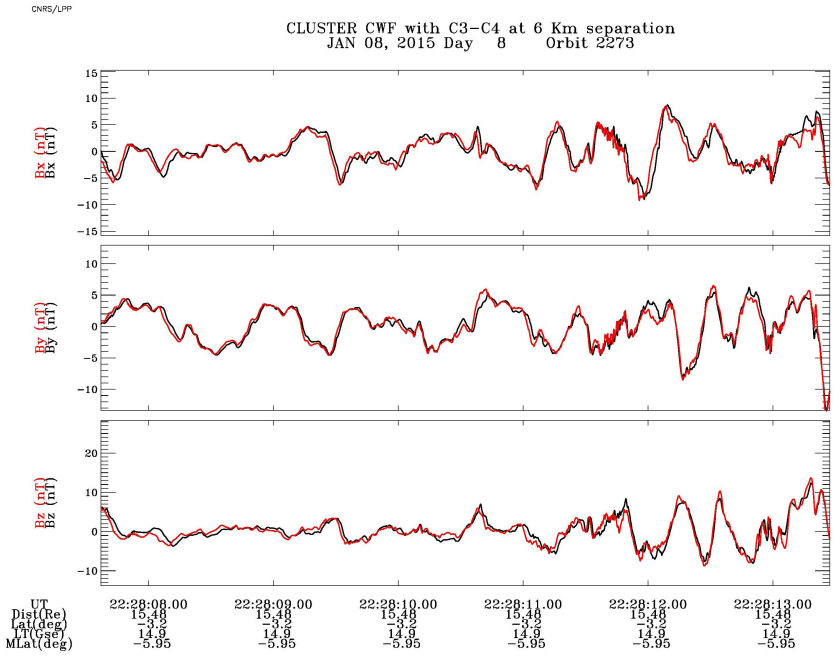

Figure 13: Superposition of waveform obtained by C3 (black) and C4(red) Separation between 2 spacecraft is ~6 km

7.1.2 STAFF–SC / STAFF–SA: spectra continuity

Figure 14 below illustrates the connection between STAFF-SC spectrum upper frequency band and STAFF-SA spectrum lower frequency band, which overlap between 8 and 12 Hz. Levels and slopes are rather good for all spacecraft.

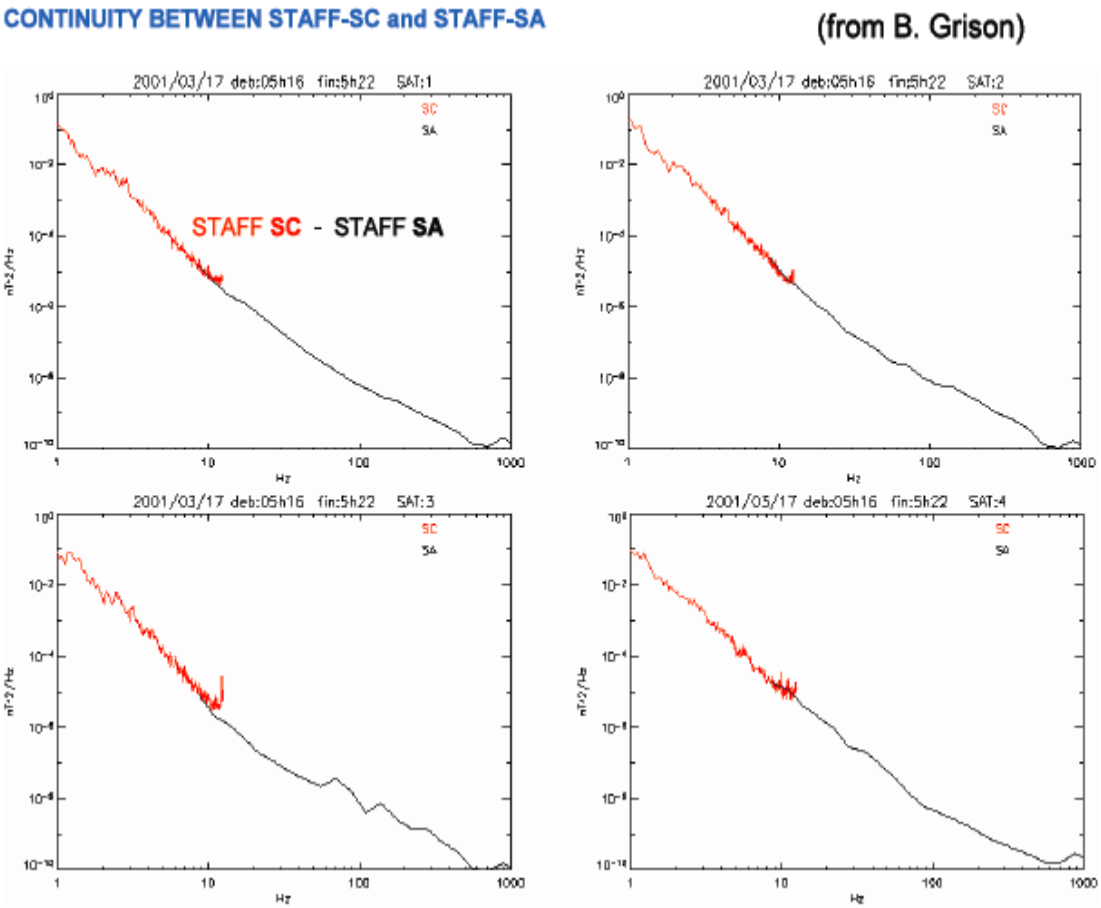

Figure 14: Spectra of STAFF-SC (red) and STAFF-SA (black)
Courtesy of B. Grison

7.1.3 Evolution of SC/SA Noise floor during the mission

This spectral continuity between SC and SA can be checked when looking for the evolution of the noise floor (sensitivity) of each instrument, and its evolution for each spacecraft over the mission duration. Figure 15 shows this evolution over 4 years (2001, 2004, 2008 and 2011) of the Bx and Bz components, between 0.1Hz to 9Hz (SC) and to 9 Hz to 4000 Hz (SA). These data were selected in regions of no or low wave activity, in the lobes, and each spectrum is an average over 3 hours of data. The sensitivity level is quite stable over the years, and the continuity between the spectra provided by the 2 instruments rather good. There is a small increase over the years in the noise level of SA band A (8-64 Hz). The interferences (see above 5.2.1) observed on SC3 and at lower level SC2, are well observed and stable.

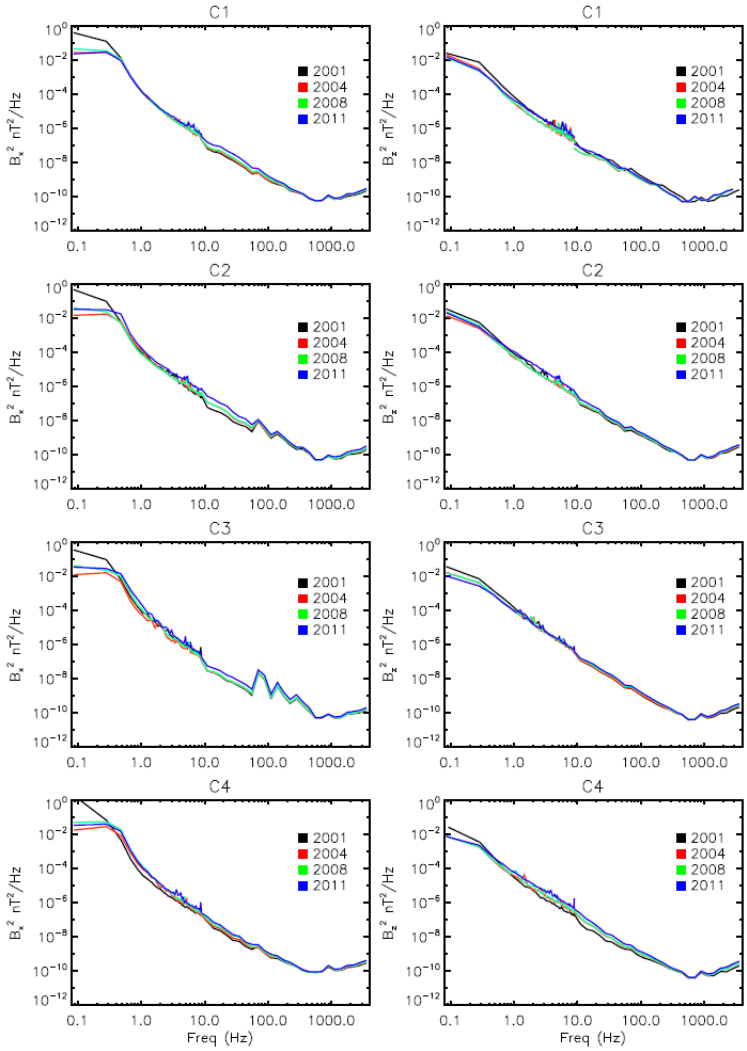

Figure 15: Evolution of sensitivity with time on combined SC and SA spectra (Bx left, Bz right)

7.1.4 SC-SA spectra continuity during special HBR mode

We can extend this comparison to higher frequencies, when SC, in HBR mode, covers the frequency range up to 180 Hz. Figure 16 (for C1) and Figure 17 (for C4) show a comparison between STAFF-SC and STAFF-SA taking benefit of a special mode commanded to get a maximum frequency overlap between the 2 analysers. The Spectrum Analyser (SA) has been commanded to provide data on all frequency bands, during a period of high telemetry rate, having then a frequency overlap between 8 and 180 Hz. The stars are for the SA frequencies, the continuous line for the result of a wavelet analysis performed on the SC calibrated waveform. The 4 plots are for the 3 magnetic components and the total power. Both behaviours are globally similar.

Courtesy of C. Lacombe and Y. De Conchy

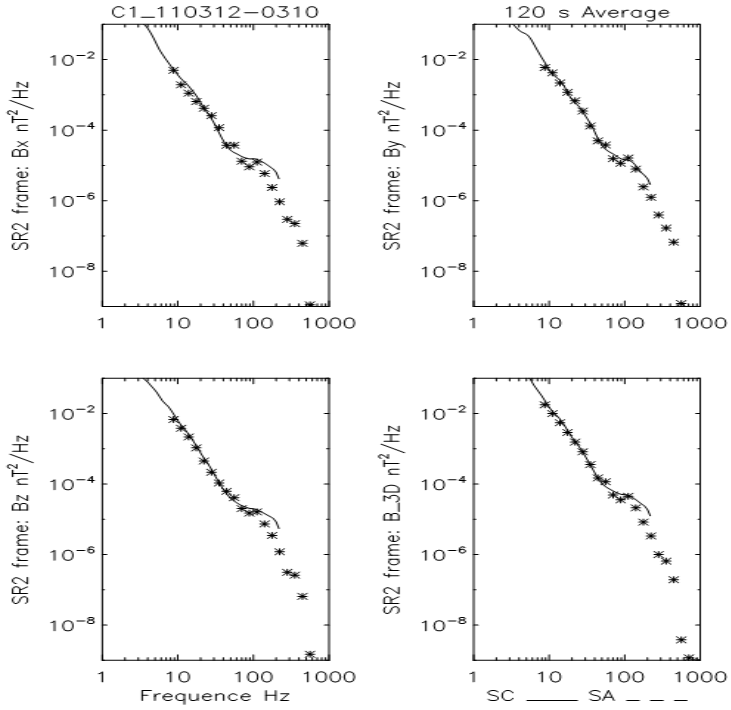

Figure 16: Combined spectra between STAFF-SC (line) and SA (crosses) for SC1

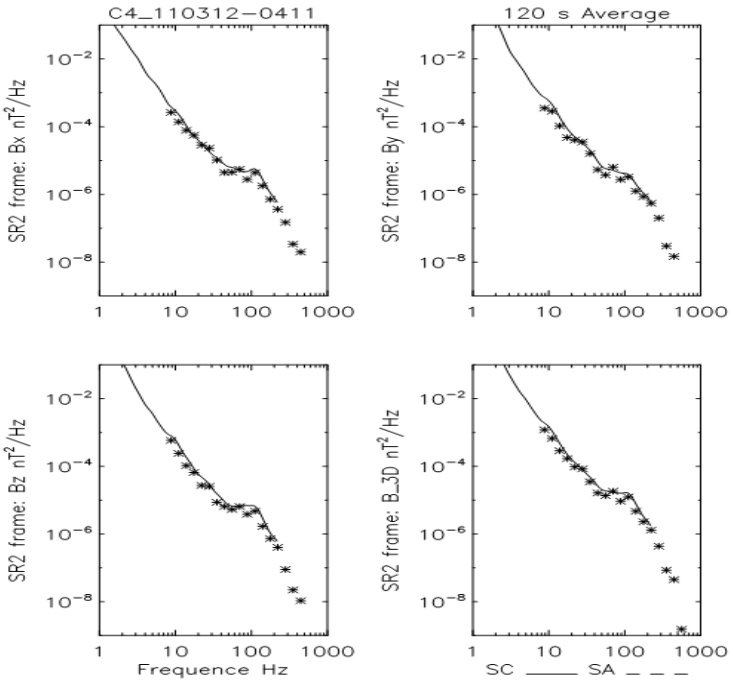

Figure 17: Same as Figure 16, for SC4.

7.1.5 STAFF–SC / STAFF–SA: statistical comparisons

For these comparisons, data from several periods have been used to widely cover the possible magnetic fluctuation intensities range. The intervals are:

- 16/12/2001 from 05:30 to 06:30 (high intensity fluctuations in the magnetosheath).
- 19/12/2001 from 02:40 to 03:40 (low intensity fluctuations in the magnetosheath).
- 03/02/2001 from 17:00 to 18:00 (very low intensity fluctuations in the solar wind).
- 19/02/2002 from 01:00 to 02:00 (low intensity fluctuations in the solar wind).

For each of these intervals, the data have been divided into 20 seconds length sub-intervals. On each of these sub-intervals, the average values have been computed around 8.8 Hz for both the STAFF-SA (SA) and the STAFF-SC (SC) fluctuations. These average values are called respectively <*sa*> and <*sc*>. Practically, the following procedure has been used.

For SA, the time resolution of each channel is one second. Therefore, <*sa*> is the average of the 20 consecutive spectral values at the first SA frequency channel, that is at 8.8 Hz. As indicated previously, the 27 SA frequency channels are distributed logarithmically in the frequency range between 8 Hz to 4 kHz. Each of these 27 channels measures fluctuations in a band Δf around a central frequency f_0 with $\Delta f/f_0 \approx 0.26$. Therefore, for the first SA frequency channel, the fluctuations are recorded over the frequency range ~7.6 to ~9.9 Hz. For SC, the PSDs spectra of the whole waveform signal are first computed on each 20 seconds sub-interval. Then, <*sc*> is the average PSD in the frequency band ~7.6 to ~9.9 Hz.

In the Figure 18 below, for each of the three components, for Cluster 1 and for all the 20 seconds sub-intervals, <*sc*> is plotted as a function of <*sa*>. On these figures the magnetic fluctuations are displayed in nT^2/Hz. The diamonds represent the magnetosheath high intensity fluctuations, the stars represent the magnetosheath low intensity and the crosses represent the solar wind data. Note that the plots and the following conclusions are very similar for all the other Cluster spacecrafts. Two main conclusions arise from this study:

- Globally the agreement between <*sc*> and <*sa*> is good while the fluctuations intensity is over $\sim 10^{-5}\ nT^2/Hz$ (diamonds). For intensities lower than this threshold (stars), there is no agreement. Only an extensive physically based study would provide us the fluctuations absolute level to determine which experiment (SC or SA) gives the true measurement. Note that this threshold value ($10^{-5}\ nT^2/Hz$) is close to the search coils (SC) sensitivity level at this frequency ($10^{-6}\ nT^2/Hz$).

- For all spacecraft, the agreement is better on the Z-component fluctuations than on the X and Y. It is probably due to the despin procedures applied to both SA and SC. For SA, the pairs of spin-plane magnetic field components are despun aboard the spacecraft. For SC, the despin is performed on the ground and has noticeable effects on the X and Y components around the spin frequency (0.25 Hz), with almost no effects on the Z component.

In summary, the agreement between STAFF-SA and STAFF-SC is good, while the magnetic fluctuation level around 8.8 Hz is over 10^{-5} nT^2/Hz. Consequently, the magnetic PSD data around this frequency, with values smaller than this threshold should be used with caution.

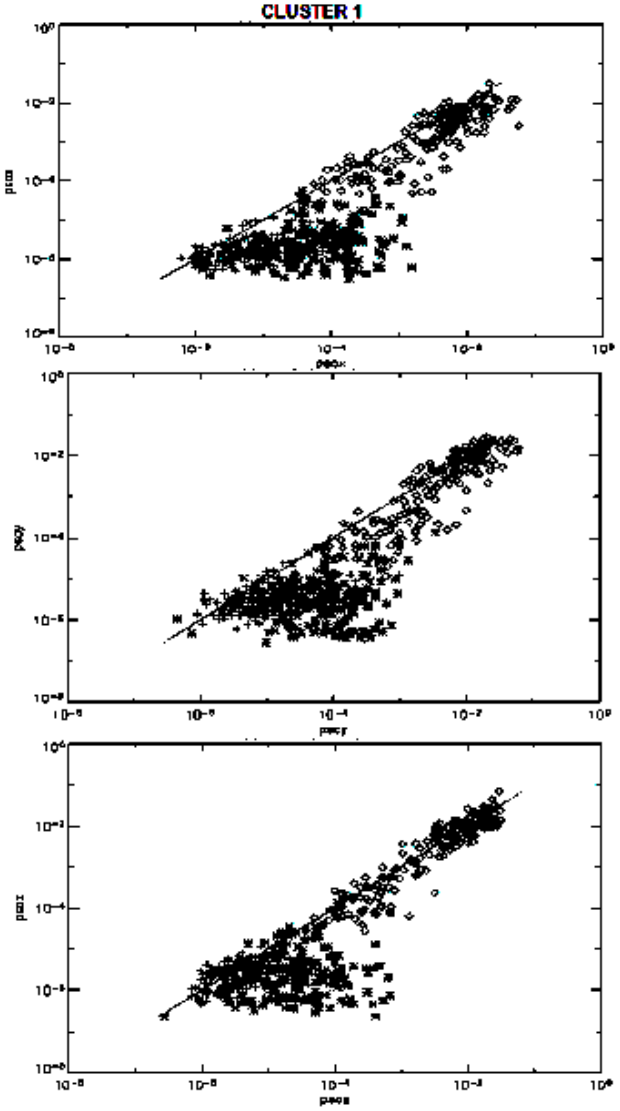

Figure 18: Comparison of magnetic fluctuations levels between SC and SA at 8.8 Hz, for low and high intensity values

7.2 Comparison between STAFF and FGM measurements

The first and evident set of data to be compared with STAFF products is coming from the magnetic field measurements provided by the Cluster FGM instrument. There are 2 sets of STAFF products which can be compared to FGM ones:

- The DC magnetic field for the Bx and By components derived from the despinning of STAFF-SC waveform as a step in the calibration process. These data are provided in the CWF in the ISR2 frame
- The magnetic fluctuations available in the CWF files where the DC components of the equatorial spin plane are removed

7.2.1 STAFF-SC / FGM: spin plane DC field comparison

7.2.1.1 Case studies

Figure 19 presents a superposition of one hour of the modulus of the perpendicular components to the spin axis of the magnetic field fluctuations ($\sqrt{(Bx^2+By^2)}$) measured in the ISR2 frame by STAFF-SC (in black) and FGM (in red) for SC1 and SC2 both obtained in NBR mode at the beginning of the mission which illustrates the very good agreement of the calibrated data products from these two instruments.

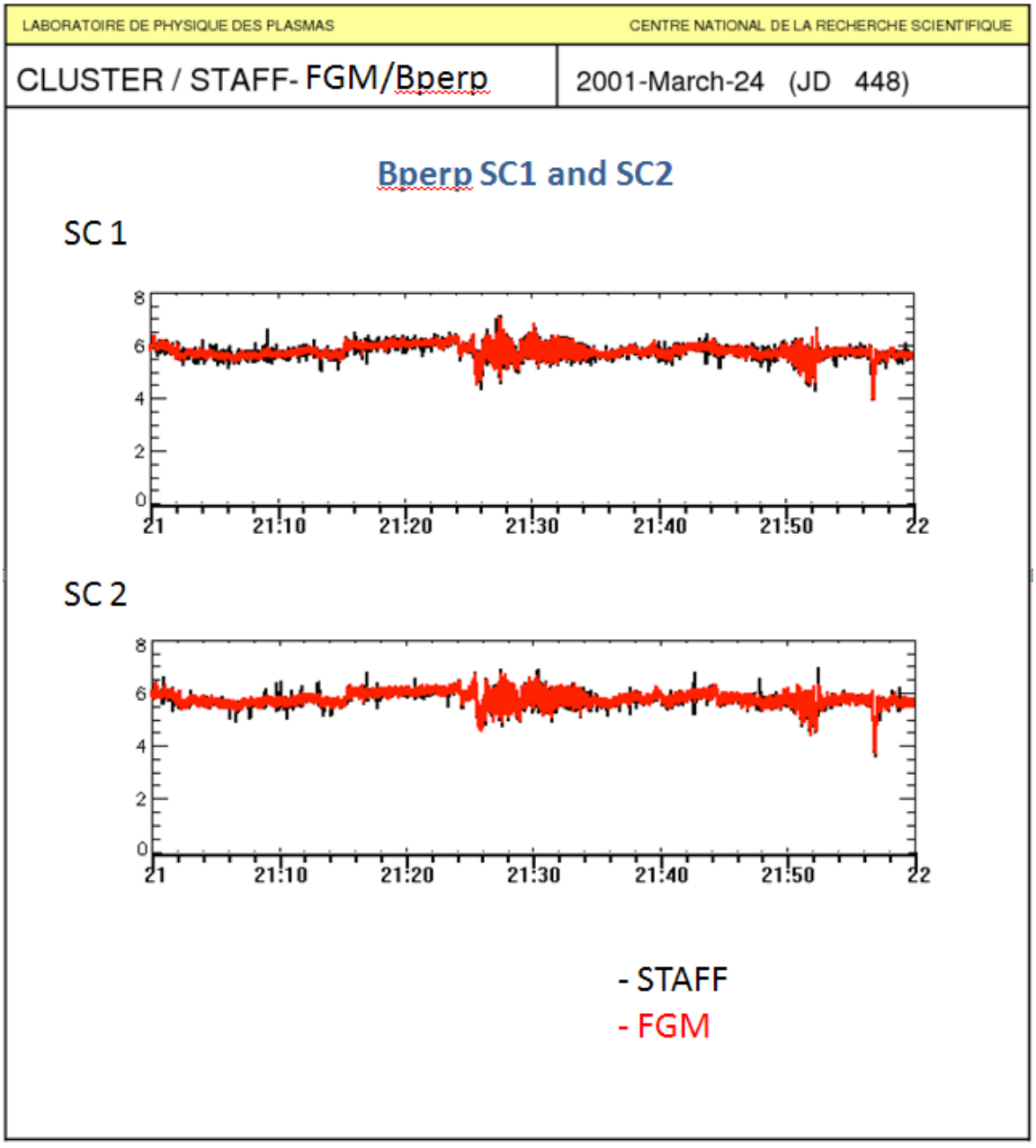

Figure 19: Comparison of the modulus of the perpendicular components coming from STAFF and FGM.

A more extended comparison is displayed on Figure 20, where Bx, By, Bperp and Phi (see Appendix A: Coordinate systems used by STAFF for the definition of φ) are superposed for SC1 and present as well a very good agreement between both data sets. Figure 21 presents the same data for SC2 with a similar very good agreement.

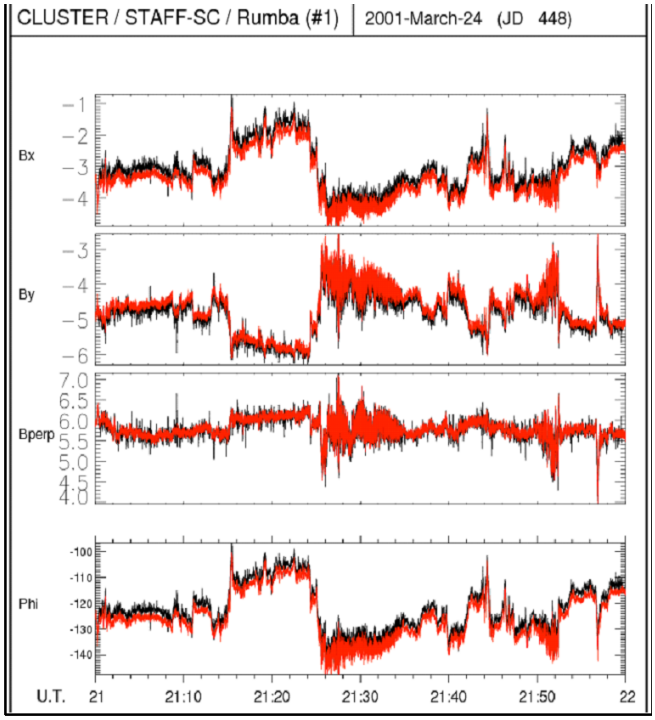

Figure 20: STAFF (black) and FGM (red) comparisons for Bx, By, Bperp and Phi components for C1.

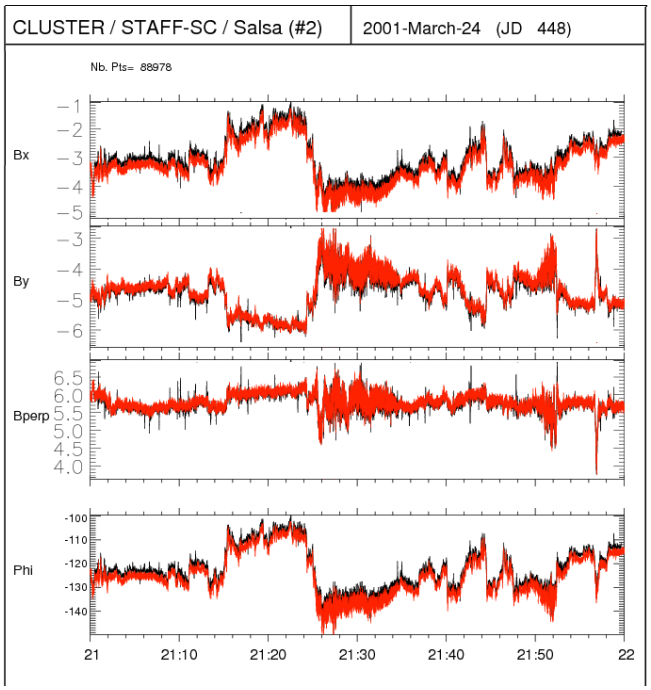

Figure 21: Same as Figure 7 for S/C 2

7.2.1.2 Statistical study for all S/C

To confirm the above results, statistics were performed over 10 years of STAFF-FGM DC field comparison. Altogether, 58 events were chosen, in four various conditions each year.

- Low DC field, low ULF activity,
- Low DC field, high ULF activity,
- High DC field, low ULF activity,
- High DC field, high ULF activity.

Results are shown on Figure 22 below (S/C#1,2,3,4 in Black, R, G, B).

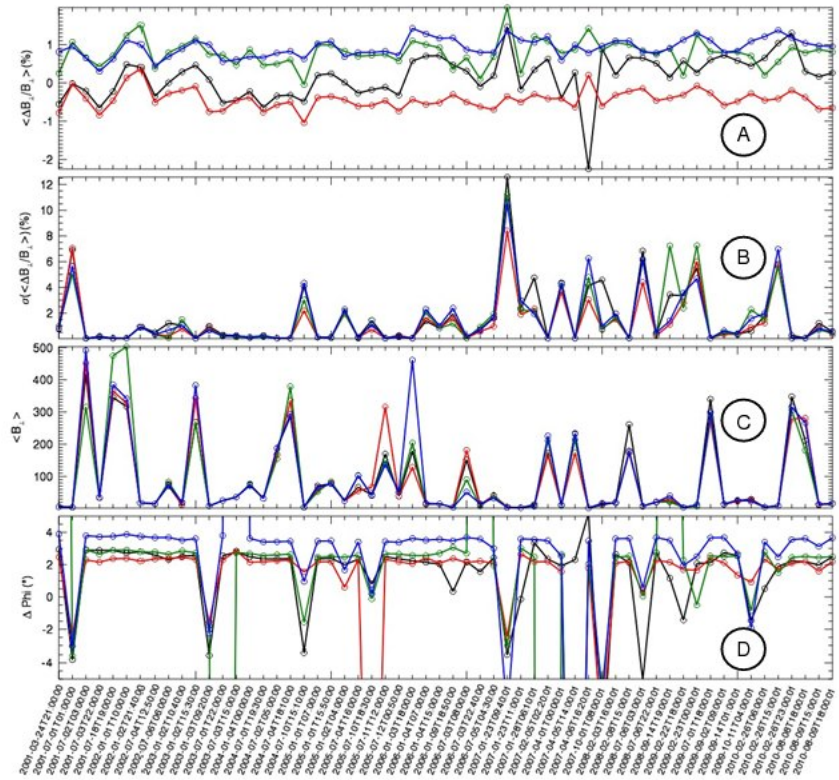

Figure 22: Statistics over 10 years of STAFF/FGM spin plane DC field
Comparison for the four spacecraft (black, red, green, and blue for spacecraft 1, 2, 3, 4 respectively)

Panel A shows the relative difference $\Delta B_\perp$ / $B_\perp$ in %, where we can see that this difference is roughly constant for each spacecraft during the 10 years studied.
Panel B shows the standard deviation of $\Delta B_\perp$ / $B_\perp$ which is between 0.5 and 5%, except for one point at 12%, but which corresponds to a very low $B_\perp$, so $\Delta B_\perp$ / $B_\perp$ becomes relatively high considering the accuracy of the measurement.
Panel C shows the amplitude of the $B_\perp$ DC field for each event, from a few nT to 500 nT.
And last, panel D gives the phase difference of the $B_\perp$ component in the SR2 system.

Concerning the relative stability of $\Delta B_\perp/B_\perp$, we can see that it is independent of the magnitude of the DC field, whatever the level of ULF activity. Furthermore, for each spacecraft, this difference remains constant all over the 10 years of this study. This good stability over time is an important result because it confirms that the transfer function remains constant from the beginning of the mission.
Another important result is the difference from one spacecraft to another. In fact, the best result seems to be obtained from S/C #1, where the transfer function has been obtained by averaging the 3 others (S/C2, 3 and 4). This result is thus directly driven by the estimate of the transfer function on the ground, and gives an estimate of their accuracy (see section 3). It has been decided to keep each of the 3x4 transfer functions slightly different, but, as these tables should be all theoretically identical, we also could have decided to set all tables to the S/C#1 average table.

Concerning the direction, most of the time this Δφ difference is between 2 and 4°. Nevertheless, for some cases, the sign of this difference changes and is between -2 to -4°. This change has not been studied.

7.2.2 STAFF-SC / FGM: waveforms comparison

The Calibrated Wave Forms (CWF) are delivered to the archive in both GSE and ISR2 frames. The figure 23 below presents an example of comparison between the magnetic fluctuations as seen by STAFF calibrated waveform (CWF) delivered in GSE to the archive (black) and FGM data (red) where both data sets were filtered to eliminate the DC components. FGM and STAFF data agree very well within 1%.

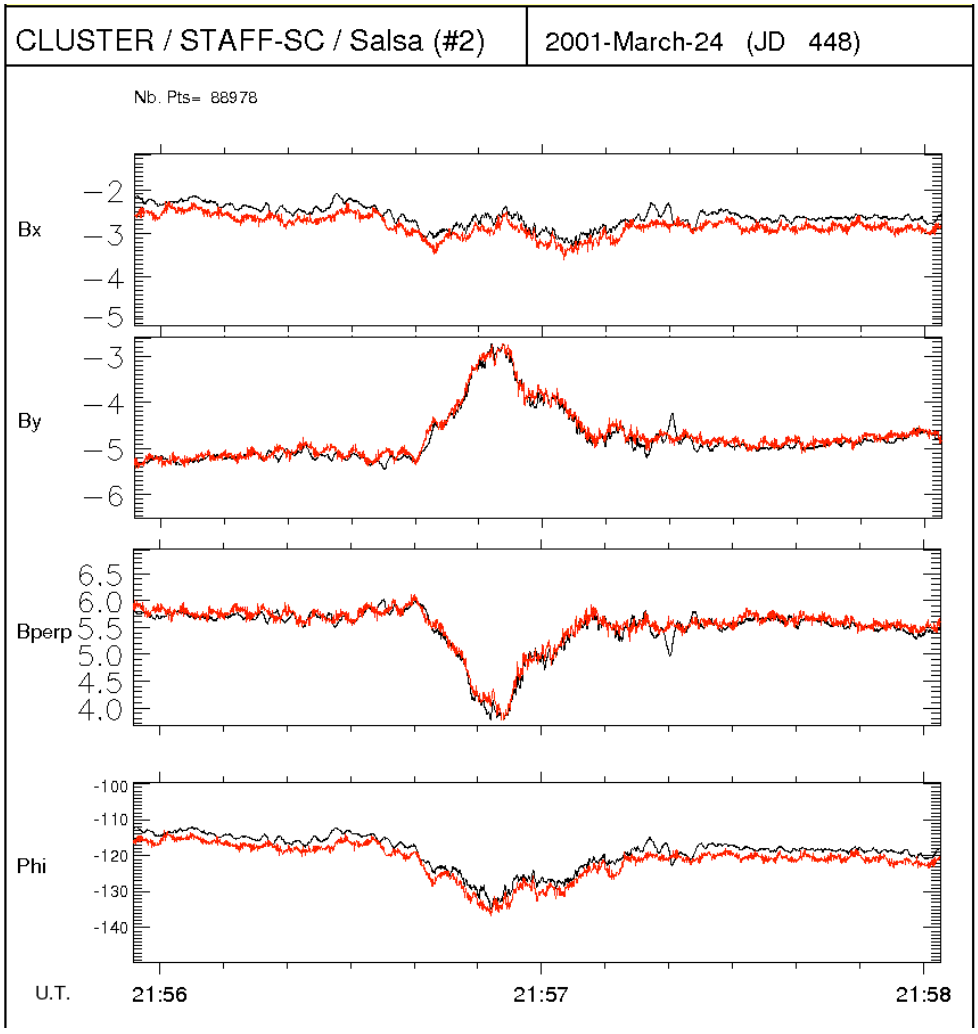

Figure 23: Comparison between STAFF (black) and FGM (red) for a short time scale event.

7.2.2.1 Comparison at 1Hz

Figure 24 shows an event with an almost monochromatic wave at low frequency (~1 Hz) superimposed to a low DC variation. The period considered is in HBR. STAFF CWF data

including the DC components in the spin plane are here compared with FGM with full time resolution. The scale has been adapted to quantify the differences. On the left, one can see a constant difference of ~1% on the $B_\perp$ component, as expected, and a phase difference of ~4°. The zoom (on the right) still shows the same agreement on the DC part, both in amplitude and phase.

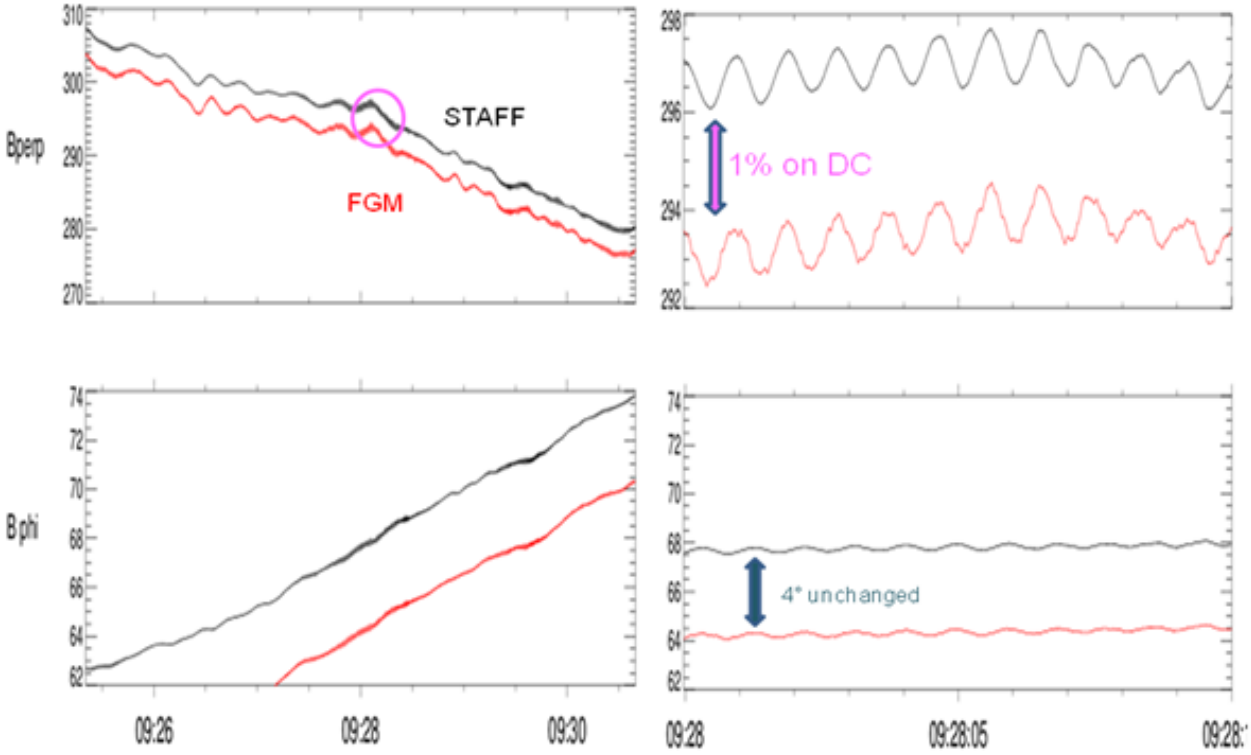

Figure 24: Comparison at 1 Hz (C4/Tango) 23 September 2001

For a more precise comparison of the component at 1 Hz, we shift the FGM data of 3.3 nT (1.1 %) to have a better superimposition of the two curves (Figure 25). The result is rather satisfying, a good fit being found, but a spectral analysis is required (next) to get a better estimate of the difference.

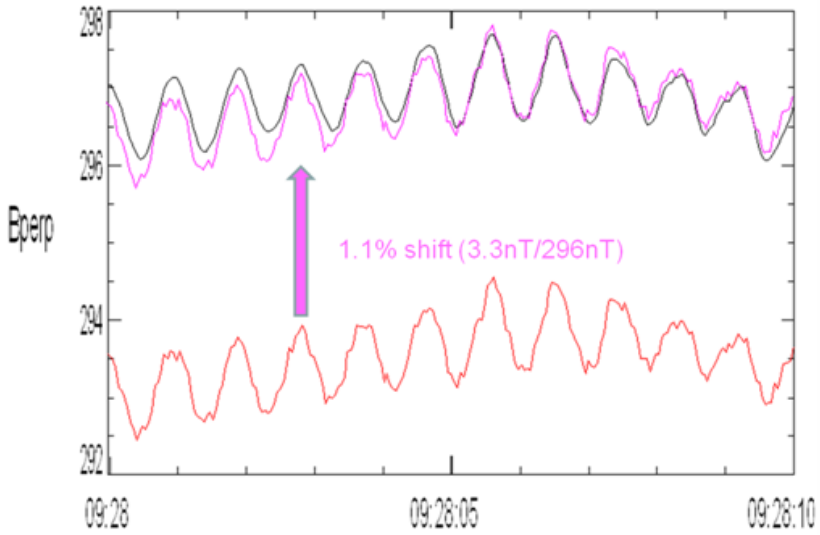

Figure 25: Wave at 1 Hz, STAFF-FGM superimposed.

7.2.2.2 Comparison at 6 Hz

The following example (Figure 26) corresponds to another almost monochromatic wave at ~6Hz this time, always superimposed to a low DC variation (The wave occurs at ~ 09:39 UT on By). The agreement on the DC field remains the same ($\Delta B/B < 1$ %, $\Delta\varphi \sim 3°$).

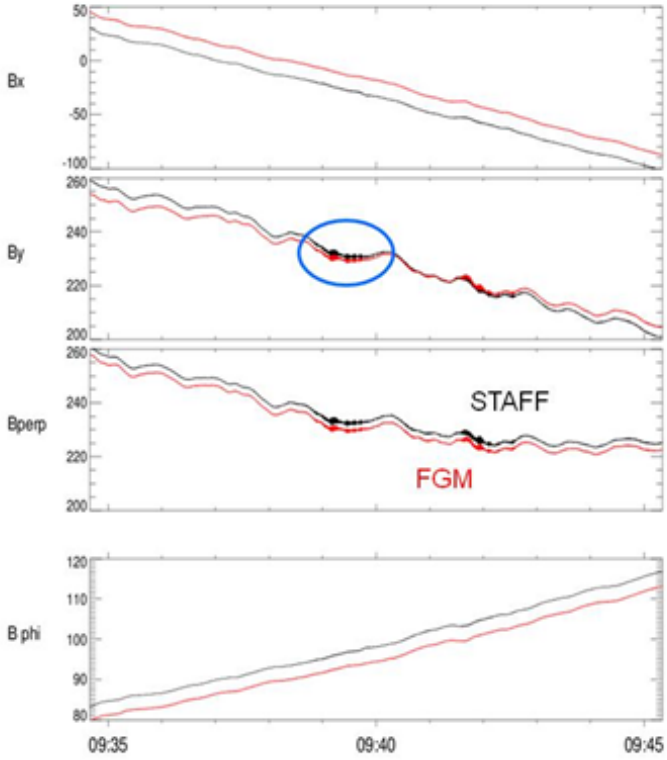

Figure 26: Wave comparison at 6 Hz (C4) 23 September 2001

By zooming on the wave (Figure 27), we can identify a ~ 6Hz wave whose both amplitude and phase appear to be in good agreement, but as previously, a spectral analysis is required to get more details. It is done in the next paragraph.

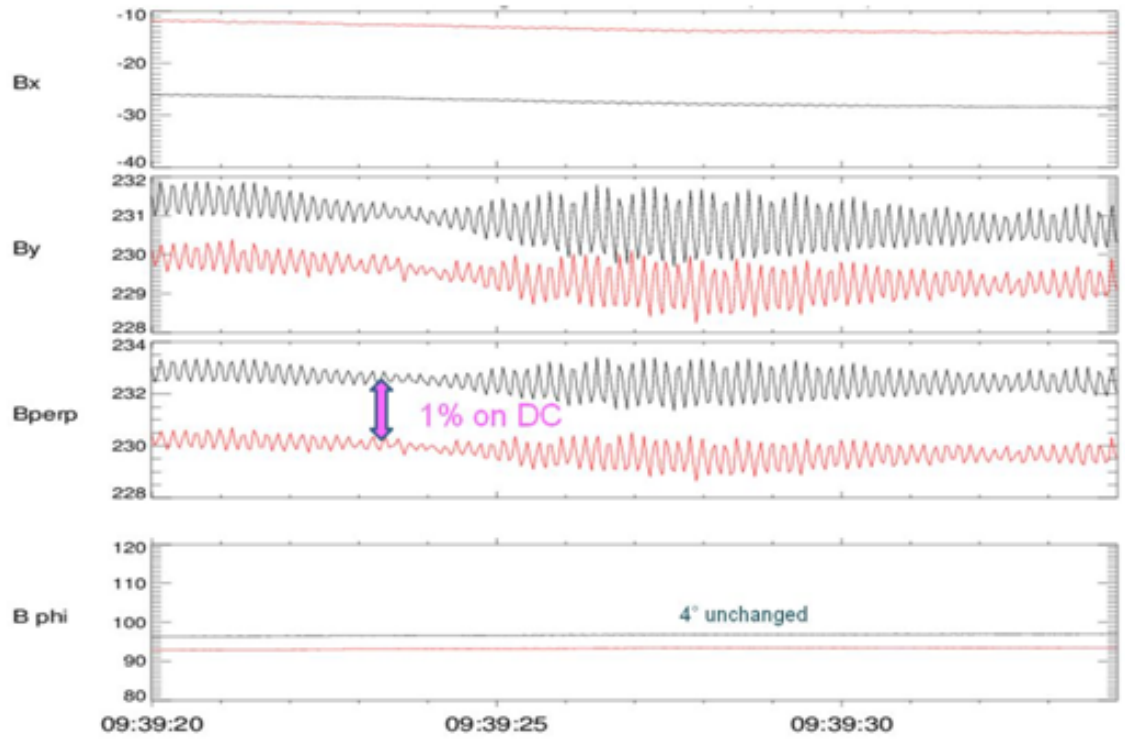

Figure 27: Zoom on wave comparison of Figure 26.

7.2.3 STAFF / FGM Spectra comparisons

7.2.3.1 STAFF-SC/FGM sensitivity

Figure 28 shows a spectrum of the Bz components for STAFF (black) and FGM (red) obtained during a very quiet period, which means that these two curves can be considered as the sensitivity of the two instruments. The STAFF ground sensitivity is plotted as a green line. The two curves (top frequency in linear scale, bottom in log scale) cross at ~ 0.7 Hz, meaning that at this frequency the two instruments have the same sensitivity. Below 0.7 Hz, FGM (in red) is not only more sensitive, but also gives the three components of the DC field, contrary to STAFF. Above 0.7Hz, the search-coils are more sensitive and can detect events of smaller magnitude. This leads to choose one experiment rather than the other, according to whether you look at the DC-field or at waves, and for which frequency range of waves you want to focus on. In fact, the two experiments are quite complementary.

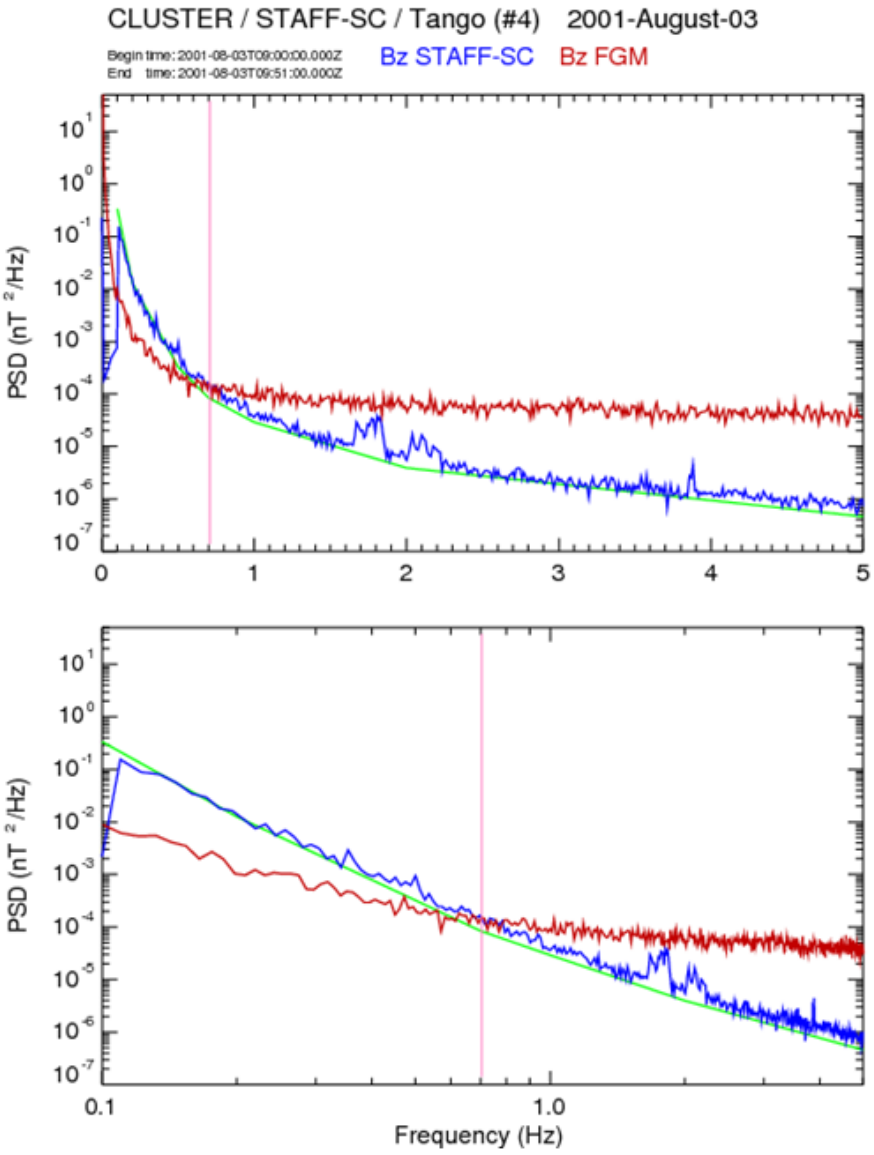

Figure 28: STAFF-SC/FGM spectra in Linear and Log Frequency scales for a very low power event

7.2.3.2 1 Hz event

Figure 29 shows the FGM and STAFF spectra corresponding to the waveform event of figure 24 and 25. The strong peak at 1 Hz spreads from 0.5 to 1.5 Hz, and the agreement between the two instruments is very good, even for the second peak at ~ 2.5 Hz. To quantify the exact difference, a dedicated study should be done, requiring filtering of the high frequencies, spikes removing and Shannon interpolation for the STAFF-FGM resampling. The noise above 3 Hz is higher for FGM, as expected; nevertheless, it is above the sensitivity shown for the wave at ~1Hz presented above.

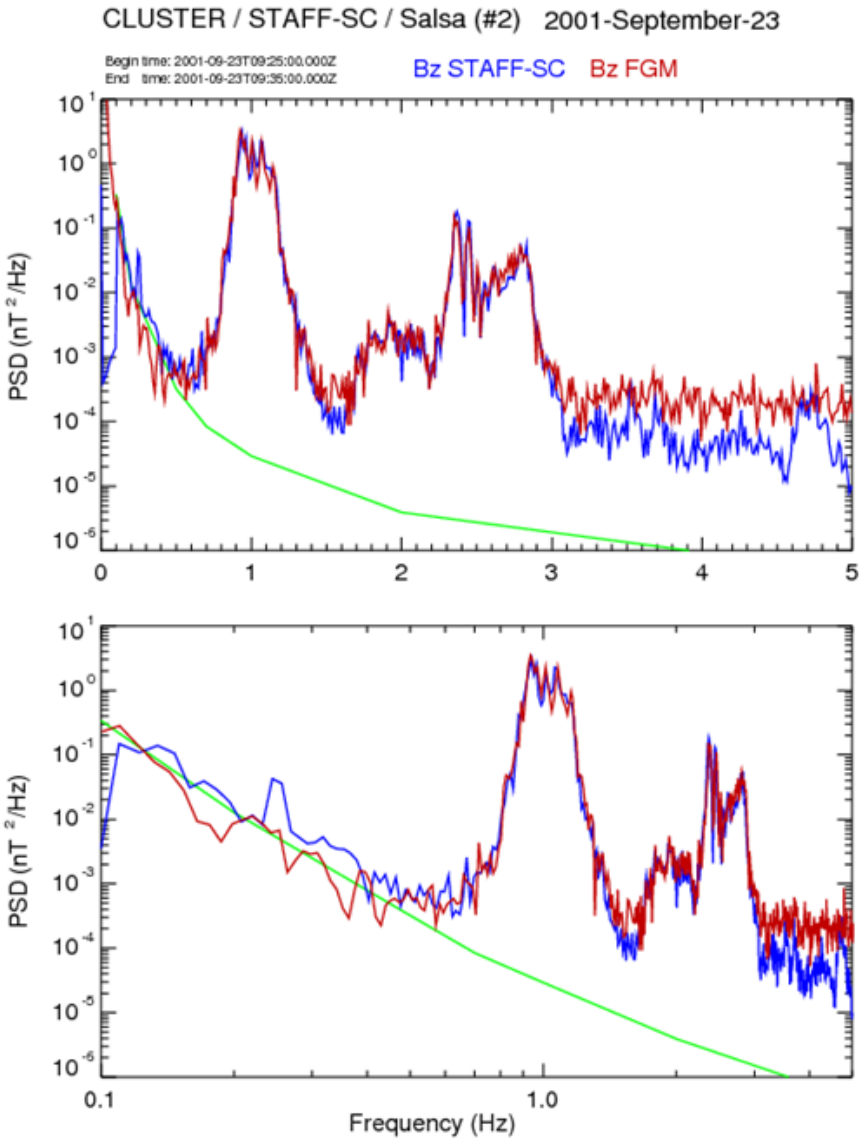

Figure 29: STAFF-SC/FGM Spectra comparison for event at 1 Hz.
Linear (top) and Log Frequency scale (below). Blue= STAFF-SC, Green=STAFF-SC's sensitivity, Red=FGM

7.2.3.3 6 Hz event

Figure 30 shows the spectra corresponding to the waveform event at 6Hz of Figure 26 and Figure 27. As above, the strong peak at 6 Hz spreads from ~ 4.5 to 6.5 Hz, and shows a very good agreement between STAFF and FGM. Nevertheless, the second peak at ~ 7.75 Hz is not recorded by FGM, its sensitivity being not sufficient at this frequency. On the other hand, low frequency below 0.4 Hz is not recorded by STAFF. This example is also a good illustration of the respective interest of the two instruments.

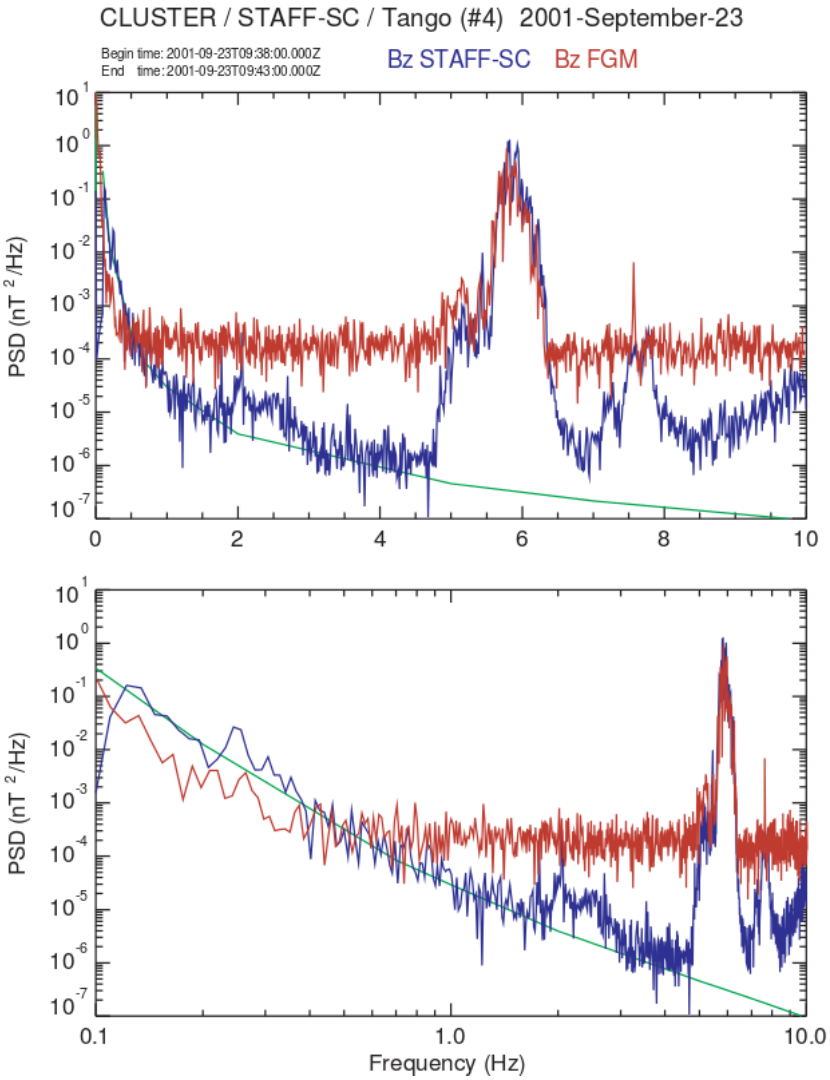

Figure 30: STAFF-FGM Spectra comparison for event at 6 Hz. (Blue= STAFF-SC, Green=STAFF-SC's sensitivity, Red=FGM)

7.2.3.4 Wide frequency band event

Figure 31 shows a strong signal over the whole frequency bandwidth in NBR. The agreement is very good between 0.1 and ~ 4 Hz. Above 4 Hz, the power spectral density (nT^2/Hz) of STAFF and FGM differs by nearly a factor of 2. Since the event is strong, the two instruments are widely above their sensitivity (the green line represents the STAFF-SC sensitivity). Furthermore, it is STAFF which is above FGM. A deeper study has not been done to explain this.

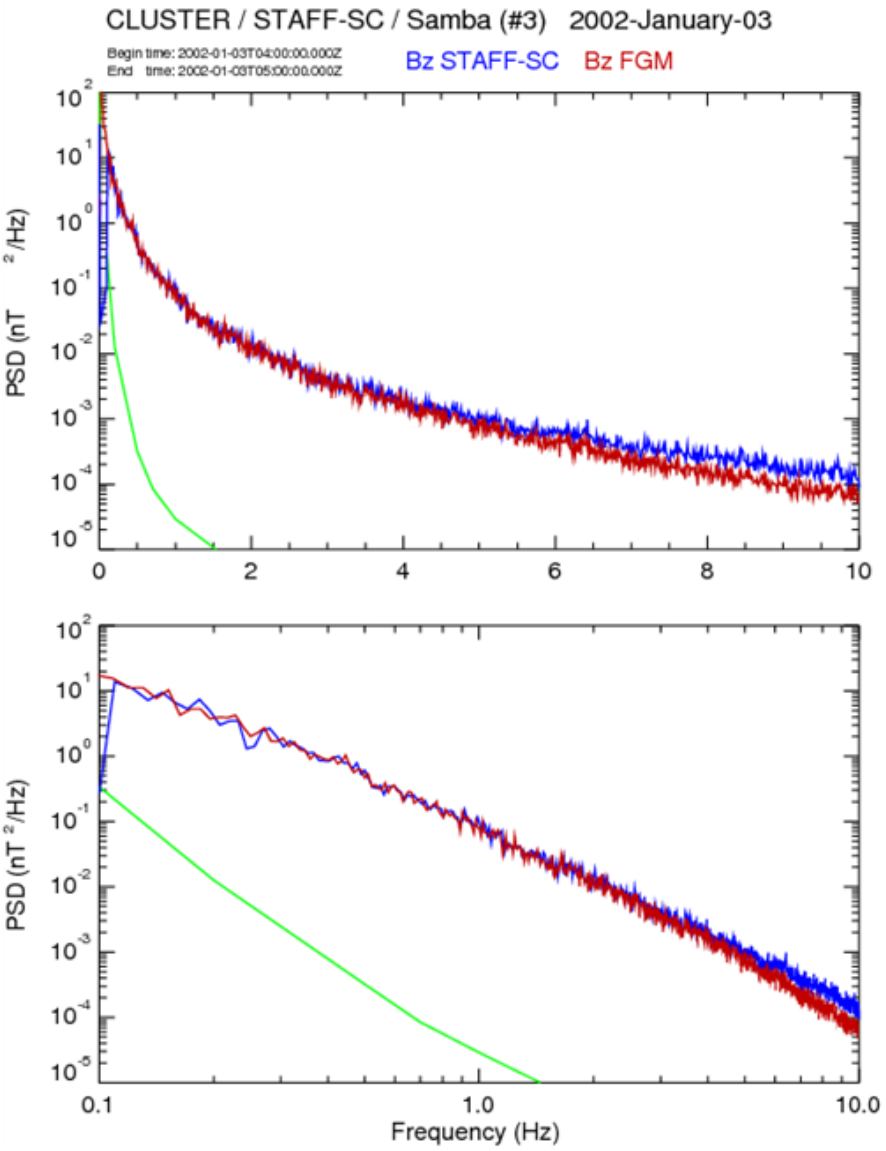

Figure 31: STAFF-FGM Spectra comparison for a large frequency band event. (Blue= STAFF-SC, Green=STAFF-SC's sensitivity, Red=FGM)

7.2.4 STAFF-SC / FGM: spectrum continuity

A further example come from a published study [9] obtained at the beginning of the mission, and show a rather good agreement between the spectra slopes of STAFF-SC (NBR) and FGM, within a common frequency range of about 0.6 to 3 Hz. These plots also show an abrupt change of the slope around 1 Hz, but the spectra continuity between STAFF and FGM is clearly visible. Although the logarithmic scale does not allow the estimation of the differences with accuracy, as previously said, the result is still significant.

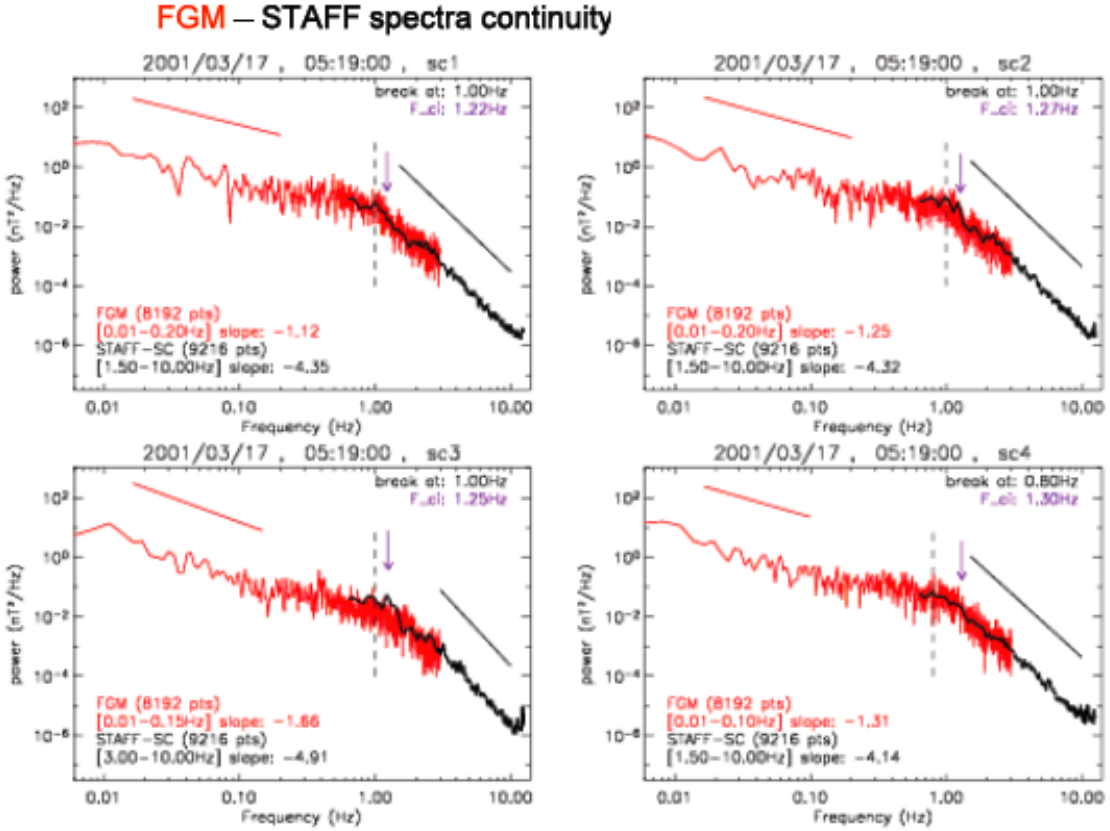

Figure 32: Comparisons of spectra coming from FGM (red) and STAFF-SC (black)

7.2.5 Choice between STAFF-SC / FGM and Merging of the 2 data sets

There is a significant overlap between the FGM and STAFF instrument capabilities for studying magnetic fluctuations, DC to about 10 Hz for FGM, 0.1 Hz to 12 Hz (in NBR) for STAFF, and the user can question which instrument has to be consider for studying magnetic fluctuations in this frequency range. The cross-calibration results presented above (7.2.1) suggests the following choice:

Frequency range / Instrument	0.1-0.5 Hz	0.5-1 Hz	1 – 10 Hz B < 10 -4 nT^2 Hz^{-1}	1 – 10 Hz B > 10 -4 nT^2 Hz^{-1}	> 10 Hz
FGM	X	X		X	
STAFF-SC		X	X	X	X in HBR
STAFF-SA					X

Below 0.5 Hz, the STAFF-SC is strongly affected by the spin frequency (~0.25 Hz). Above 10Hz, the FGM values can be underestimated because of the transfer function of the instruments, and can be subject to some interferences (se FGM CR [3]).

For some studies, like mentioned above in 7.2.4, it could be very interesting to merge the 2 calibrated data sets to get the best of each instruments, in the range DC-12 Hz. This is technically possible, and has been done by different teams (EFW, FGM, MMS, …), with a software that:

- Resamples the 2 data sets to have same periodicity in the merged set
- Low pass filters the FGM data
- High pass filters the STAFF-SC data
- Adds the 2 data sets

A key point in this process is to select a *cross-over frequency* to be used in the low/high pass filtering of the two data sets. A possible choice could be the 1 Hz frequency, which corresponds to the crossover frequency of the sensitivity of the two instruments illustrated above. Below this frequency, the FGM provides the best results, mostly free from spin frequency impacts. Above this frequency, STAFF can detect emissions that are below the sensitivity of the FGM. The two instruments agree quite well for waves above this threshold of the FGM.

However, there are some limits to consider in using STAFF CWF for merging with FGM data:

- The comparisons illustrated above have been checked only on a few examples.
- CWF relies heavily on a good despin of the raw data, obtained from parameters (window size) providing good results in average, but can produce poor quality data when large fluctuations are observed on time scale shorter than the spin rate.
- The good quality of despin, checked over many examples and many years of observations (i.e. Figure 22), have not been systematically checked for data obtained in regions key for Cluster Science (shock, magnetopause, currents, …) with potential high-speed variations in the plasma parameters.

Thus, although it is technically possible to produce a merged dataset for the data collected during the entire Cluster mission, this was not done for the CSA given the high risk of obtaining a large number of anomalies in a production that could not be systematically validated.

Of course, the interested user can produce such a merged file from a limited data set, and decide about the most relevant cross-frequency value, after checking the context of observations, any Caveats associated with each data set and the quality of data against the limitations listed above.

7.2.6 STAFF-SC/ FGM comparisons: conclusions

The calibrated data coming from STAFF-SC and FGM are in very good agreement, both for the DC values obtained, the waveform amplitude (~1-2 %) and phase (2-3%) as well as for the spectra derived from these waveforms and the continuity in frequency of these spectra on their respective range.

7.2.7 Limitation of STAFF-SC / FGM comparisons at low frequency

The DC part of the magnetic field can be estimated by STAFF-SC thanks to the Doppler effect, as seen previously. But, since the transfer function is null at zero frequency, there is a gap in the observed spectrum, depending on the wave polarization.

So, a right-handed polarized wave at spin frequency cannot be recorded by the STAFF sensor. It is seen at F=0 by the spinning sensor coordinate system because we have $F_{SR2}= F -F_{spin}$

But a left-handed polarized wave at any frequency, including DC, is recorded by the STAFF sensor because its frequency is $F_{SR2}= F +F_{spin}$

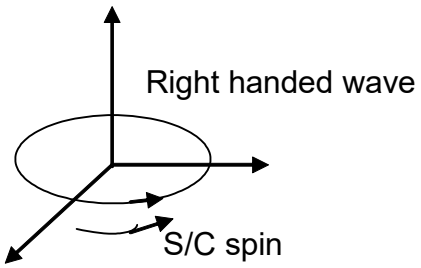

Figure 33

In conclusion, at low frequency, near the spin frequency, we cannot expect a full agreement between STAFF and FGM, except for left-handed polarized wave. This is why the CWF will be filtered below 0.6 Hz in the GSE frame, in addition to the need to avoid the strong signal near the spin frequency, to get data with a good accuracy.

7.3 STAFF–SC / STAFF–SA and FGM: continuity

Figure 34 below shows a combination of FGM, STAFF-SC and SA data for magnetic and STAFF-SA and EFW for electric components. A good continuity is observed between the data sets, acquired during a magnetopause crossing, with a rather constant slope up to 200 Hz. The STAFF sensitivity is also plotted.

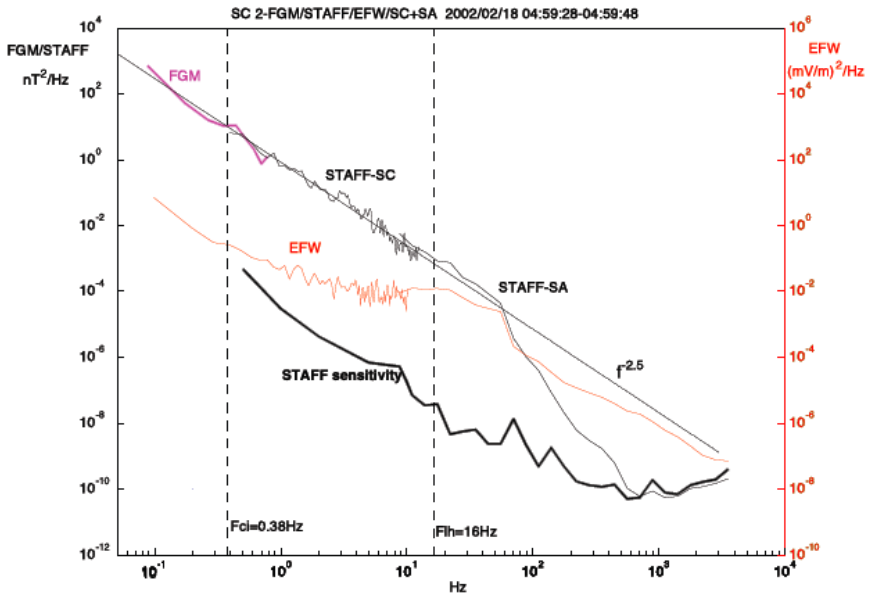

Figure 34: Combination of FGM, STAFF-SC and SA spectra

7.4 Comparison of STAFF–SA with other WEC instruments

Here are presented cross-calibration results between STAFF and other WEC instruments. First, comparisons of magnetic fluctuations between STAFF-SA and WBD, then between STAFF-SA electric field fluctuations and EFW, WHISPER and WBD. Since the comparisons between STAFF-SA and WBD have been done on a reduced data set, they are probably not fully representative.

7.4.1 STAFF-SA and WBD: magnetic fluctuations comparisons.

A chorus type event detected when WBD and STAFF-SA were both operating has been chosen (see below Figure 35)

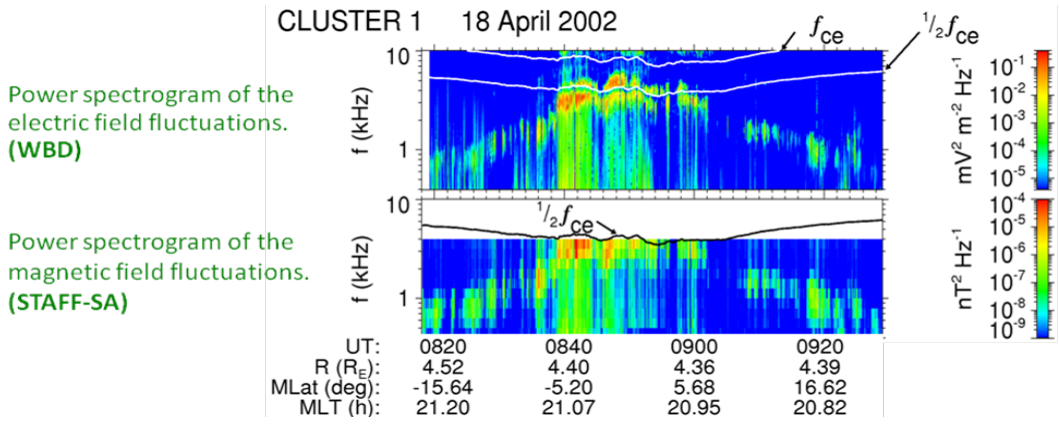

Figure 35: Comparison between STAFF-SA and WBD spectrum

The analysis has been done during the most intense part of the event, between 08:44:55 and 08:53:48. The WBD magnetic spinning component By is acquired 10 s over 50 s of data (covering periods where Whisper is active). A FFT is applied to the time series samples corresponding to the 4s STAFF-SA analysis intervals and the power is averaged over frequency intervals corresponding to the 27 STAFF-SA frequency bins. The STAFF-SA data are despun and analyzed onboard. Figure 36 shows the results of the comparison, for the whole frequency range and for the 3 STAFF-SA bandwidths.
The best fit is for band C (500-4000 Hz), which corresponds to the frequency range of the maximum wave power).

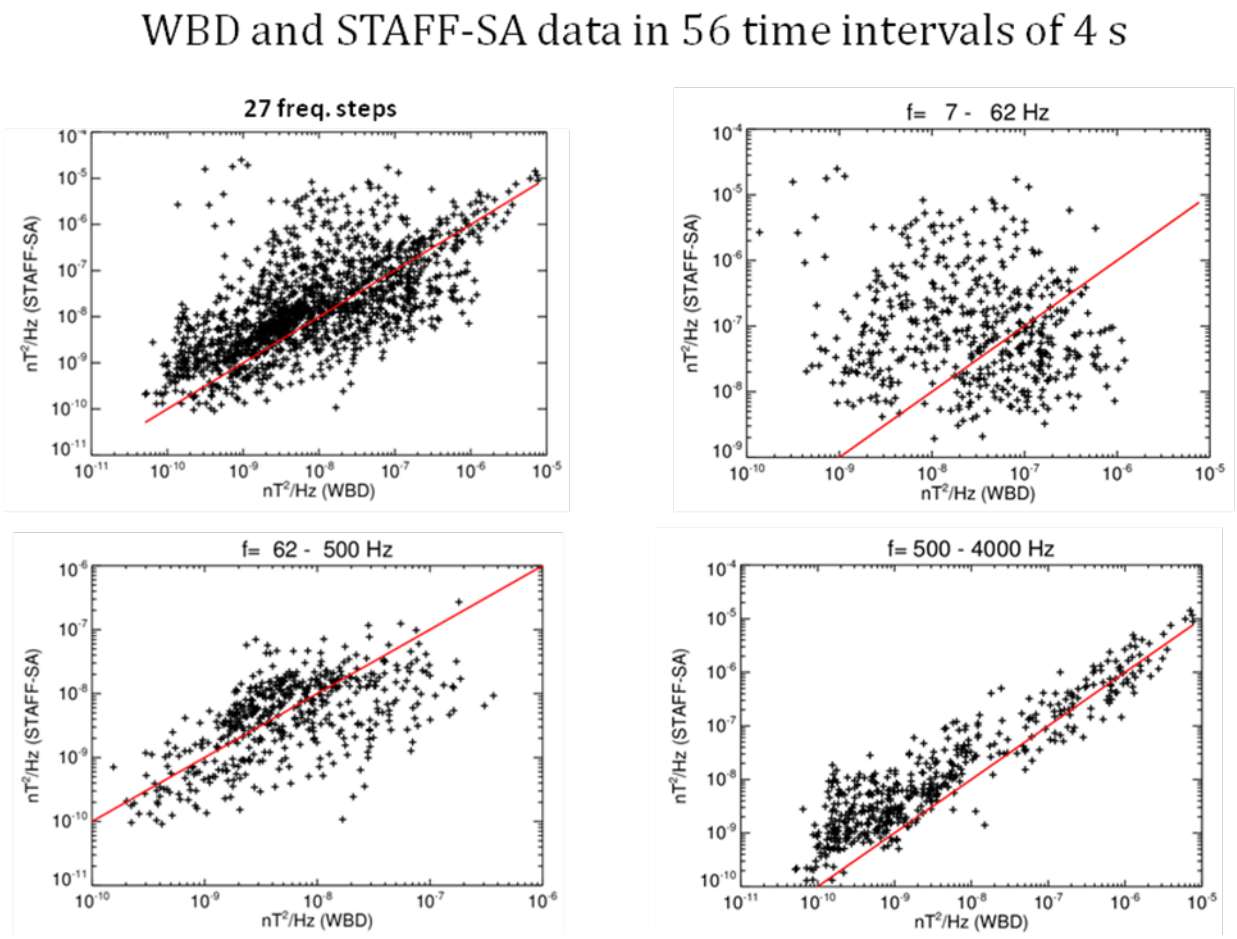

Figure 36
Comparison of STAFF-SA and WBD power density of magnetic fluctuations (in nT2/Hz) for the whole frequency range (top-left) and for the different STAFF-SA frequency bands A, B, C.

The median power ratio (STAFF-SA/WBD) is shown in Figure 37. For strong waves the ratio is about 4 in band C, about 1 for low amplitude waves (band B). The behavior in band A, where the signal is at noise level, seems to be linked to the WBD high pass filter.

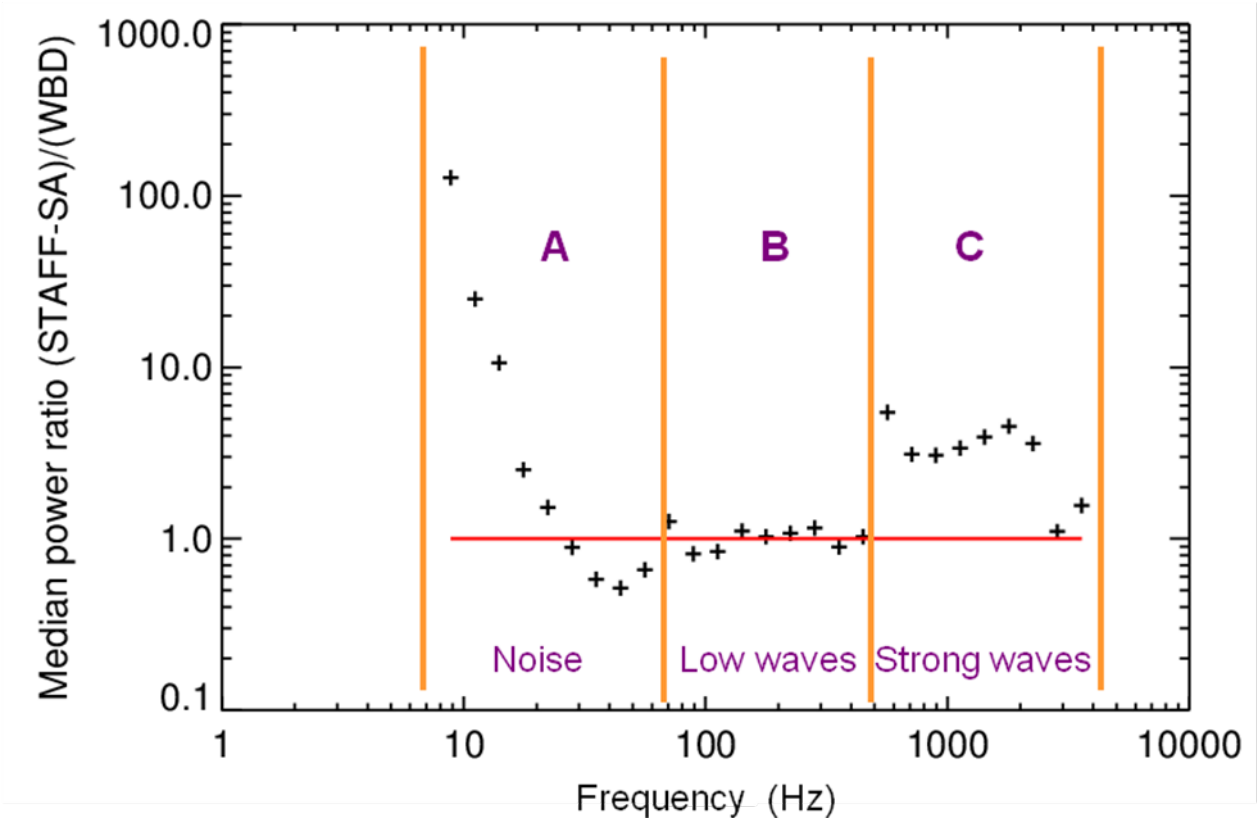

Figure 37: Plot of the median power ratio of STAFF-SA over WBD
Computed in frequency bins similar to those of STAFF-SA and over similar time periods.

For the lower frequency band A, in which there was no wave signal for the studied event, one sees the effect of the WBD high pass filter.

The above differences between the two experiments can be partly explained by the differences in the data acquisition and processing. The behavior of the background noise is explained by the WBD high pass filter. The difference between bands B and C is still to be understood. For the higher signal, the ratio of 4 in power (then 2 in amplitude), should be corrected with the revised transfer functions to be applied on the different on board analysers.

7.4.2 STAFF–SA and EFW: electric fluctuations comparisons.

For these comparisons, we have used data of two different periods, one when the spacecraft were in normal bit rate and one in high bit rate. This allows to make the comparison for two different frequency ranges, around 8 Hz and around 70 Hz.
The first period, in NBR, is on the 16/03/2002 from 05:00 to 08:00, which corresponds to a cusp crossing. For this period, data were available only for Cluster 3 & 4.

For the SA/EFW comparison, the analysis procedure approach used for magnetic component and described in the previous section has been adopted for the electric component. On the next two figures, the SA electric fluctuations have been plotted as a function of the EFW ones

in the range 7.6 to 9.9 Hz, for each of the two electric components, for Cluster 3 and for each 20-second sub-interval.

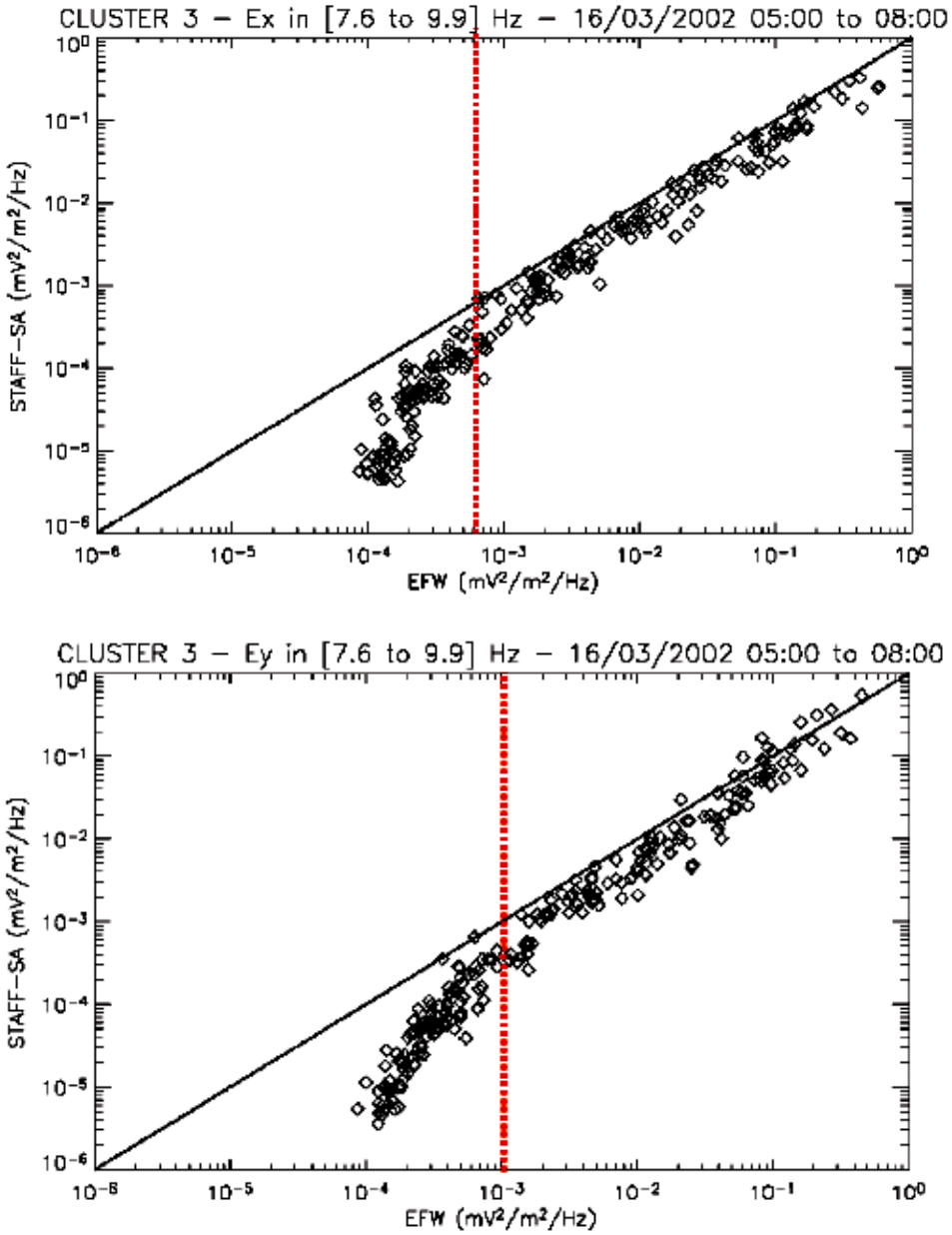

Figure 38: Comparison of STAFF-SA and EFW electric field power Frequency ~ 8.8 Hz in NBR mode for the Ex (top) and Ey components (bottom).

For the HBR comparison, the results plotted in Figure 39 correspond to an hour of data of C2 on 2001, April 19th.

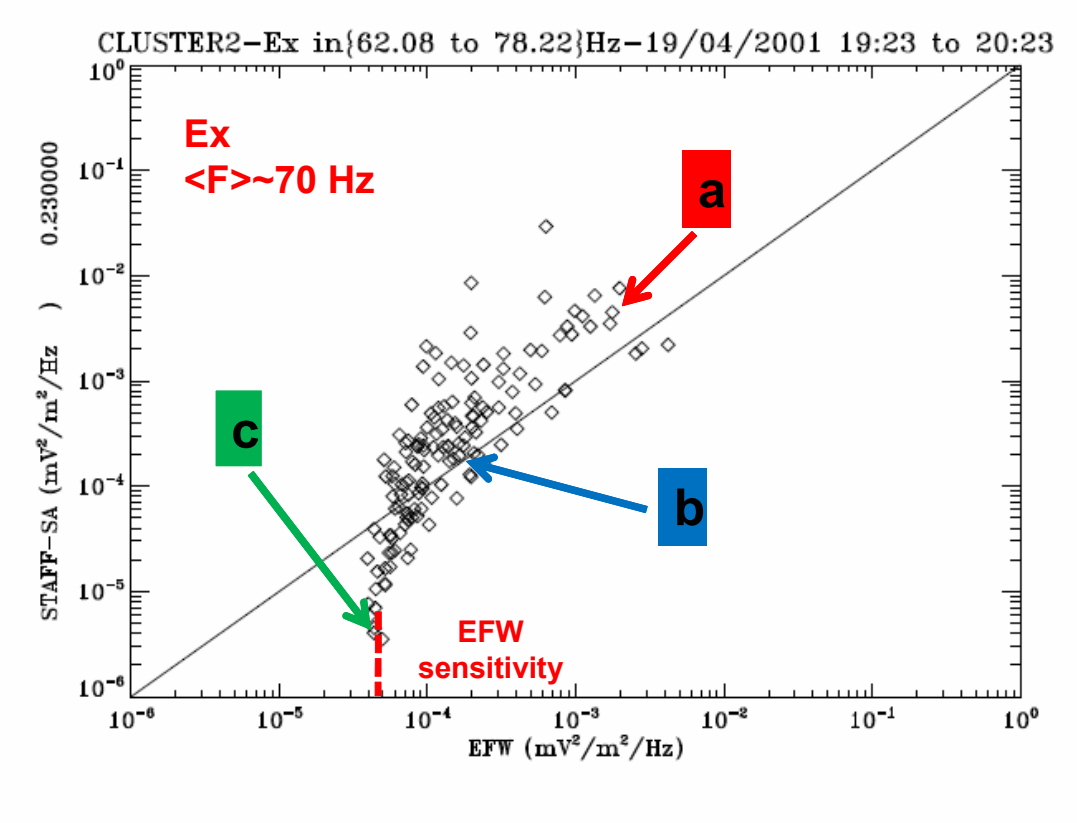

Figure 39: Comparison of STAFF and EFW electric components in HBR mode.

On the three previous figures, the electric fluctuations are displayed in $(mV/m)^2/Hz$. The data are globally in good agreement when the intensity of the fluctuations is over a given threshold. For the four spacecraft, this threshold is $\sim 10^{-3} (mV/m)^2/Hz$ around 8Hz and $\sim 10^{-4} (mV/m)^2/Hz$ around 70 Hz. Below these thresholds, the two experiments disagree. It is probably due to the EFW sensitivity level which reaches these values at these frequencies [A. Ericksson, private communication].

Conclusion of the STAFF-SA/EFW comparisons: the agreement is good while the electric fluctuations level around 8.8 Hz is over *6 to 10 x* 10^{-4} *$(mV/m)^2/Hz$*. As this latter value is known to be close to the EFW experiment sensitivity, the electric PSD data, around this frequency, should be retrieved preferentially from the STAFF-SA experiment. In the same way, in high bit rate, if the fluctuations level around 70 Hz is below *6 to 10 x* 10^{-5} *$(mV/m)^2/Hz$*, one should preferably use SA data.

7.4.3 STAFF–SA, WHISPER and WBD: electric fluctuations comparisons.

A first comparison between those three instruments measurements is given in Figure 40. On this figure are displayed the electric field fluctuations measured at the same time by STAFF-SA, WHISPER and WBD. Depending on the frequency overlaps, the agreement varies between the three experiments.

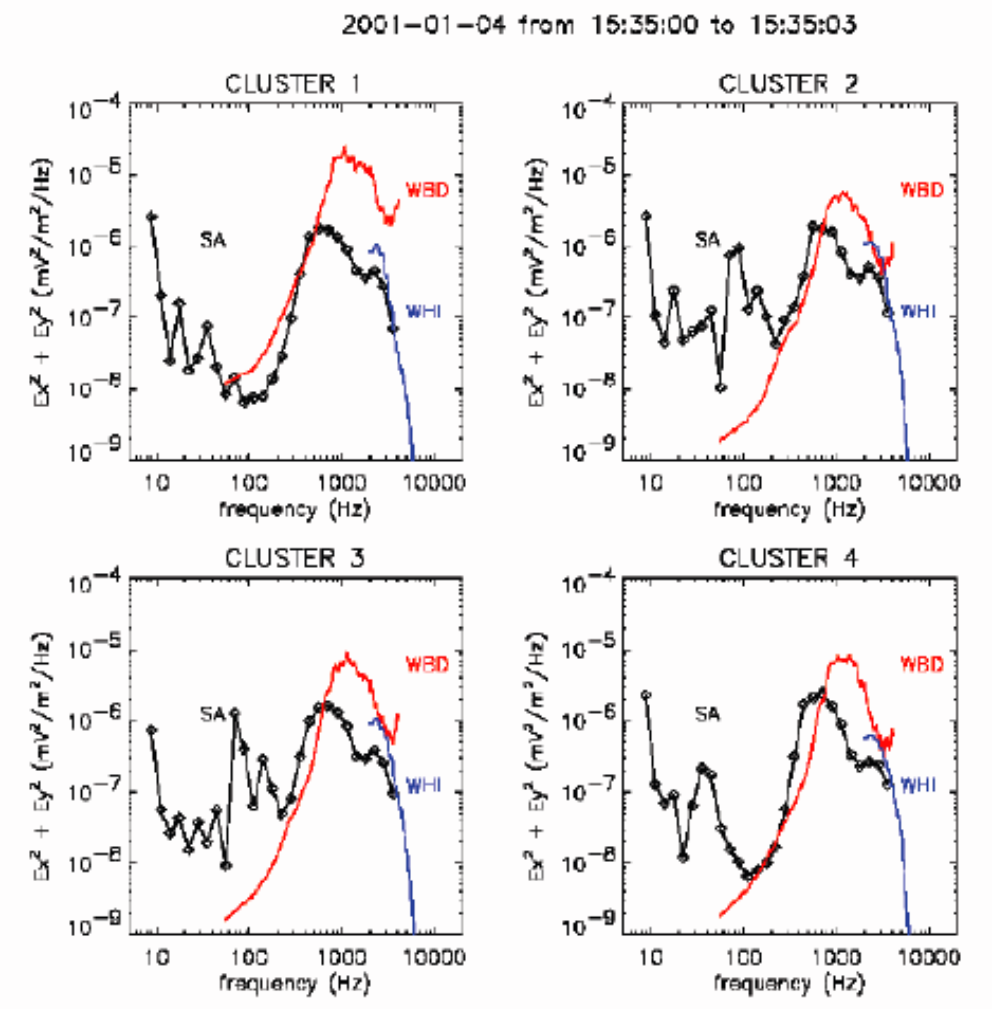

Figure 40: Comparison of results from the STAFF-SA, Whisper and WBD instruments
A single event is considered for the 4 spacecraft. Significant discrepancies are observed

There seems to be good agreement between Whisper and WBD (except on C1), but the WBD/STAFF comparison shows unexplained discrepancies. The understanding of these significant differences will have to consider the differences in how these instruments collect their data.

A final comparison is done using STAFF-SA and Whisper data on longer time intervals:

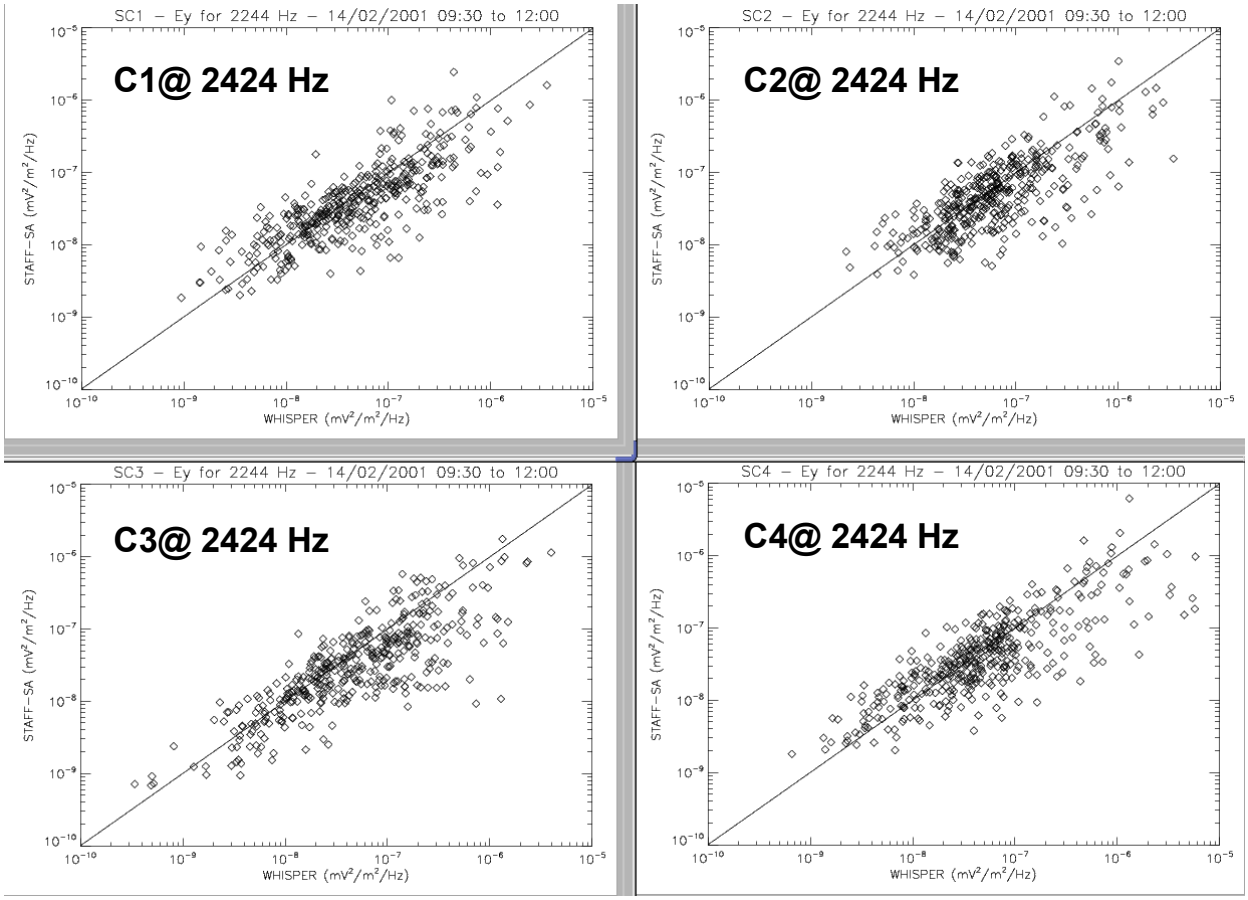

Figure 41: Comparison of STAFF-SA and Whisper (medium intensity).

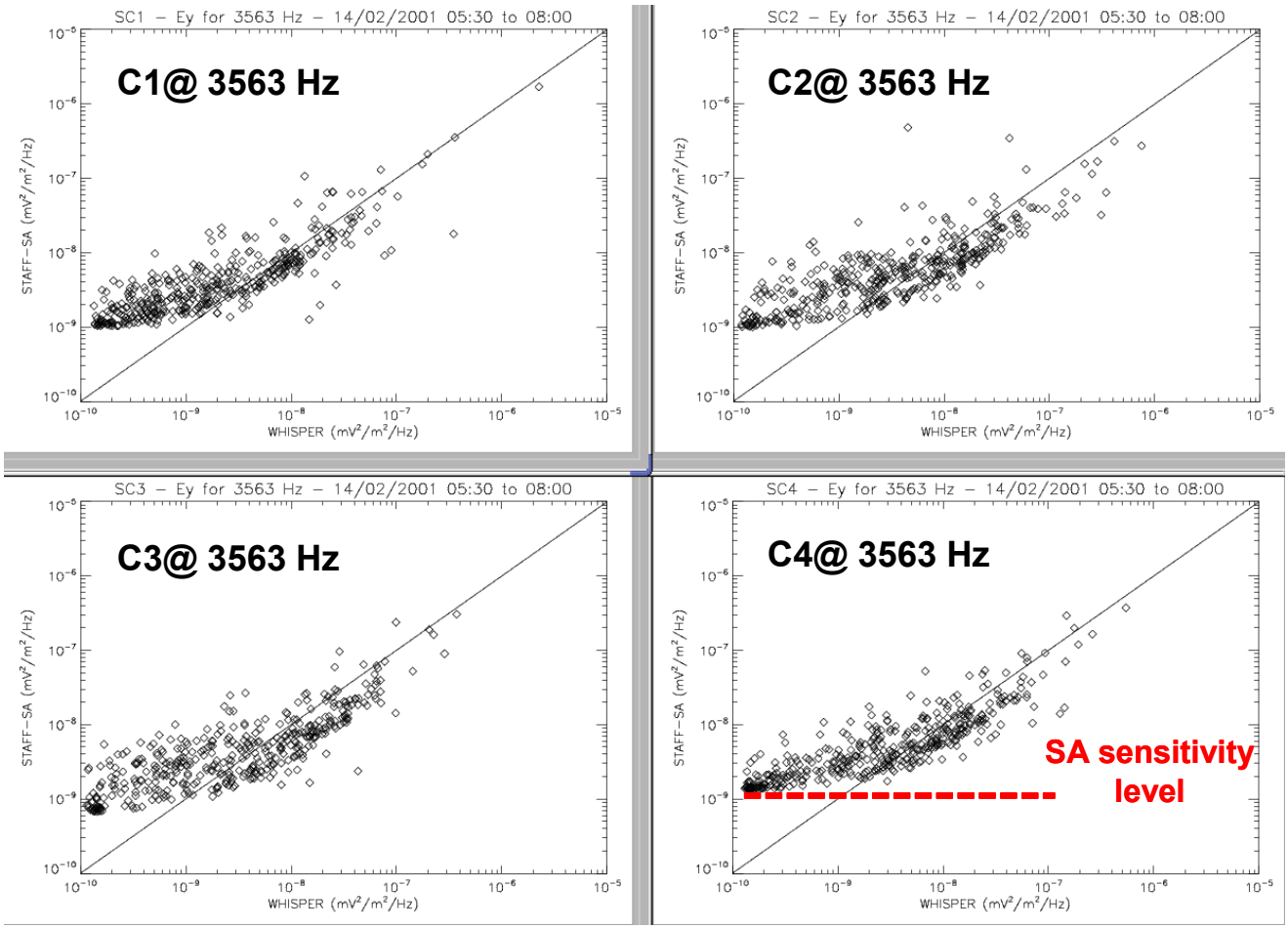

Figure 42: Comparison of STAFF-SA and Whisper (low intensity).

This comparison is done on 2 different frequencies channels and different regions. Figure 41 displays data collected close to the magnetopause with medium wave intensities, while Figure 42 shows data collected in the plasmathrough with lower level intensities. The agreement between the 2 instruments is rather good on the first example, and presents a significant difference for the lower level intensities, which can be attributed to reaching the sensitivity level for STAFF-SA.

In conclusion, the agreement between SA and WHISPER is quite good. Nevertheless, at high frequency (~3500 Hz) the sensitivity level of STAFF-SA is not as good as the Whisper one.

8. References

[1] Nicole Cornilleau-Wehrlin; Chauveau, P.; Louis, S.; Meyer, A.; Nappa, J. M.; Perraut S.; Rezeau, L.; Robert, P.; Roux, A. and C. De Villedary: **The cluster spatiotemporal analysis of field fluctuations (STAFF) experiment**. *Space Science Review* **79**: 107- 136, 1997.

[2] N. Cornilleau-Wehrlin, C. Burlaud, **"User Guide to the STAFF measurements in the Cluster Science Archive (CSA)",** ESA CSA-EST-UG-001.

[3] C. Carr, P. Brown, L.-N. Alconcel, T. Oddy, P. Fox, **Calibration Report of the FGM Measurements in the Cluster Science Archive (CSA),** CAA-EST-CR-FGM, 2015

[7] C. C. Harvey, Belkacemi, M., Manning, R., Wouters, F., de Conchy, Y.: **STAFF Spectrum Analyzer, Conversion of the Science Data to Physical Units.** Technical Report OBSPM-N-0001, issue 7, rev. 5, Observatoire de Paris Meudon.

[8] Santolik O., **"Propagation Analysis of STAFF-SA Data with Coherency Tests (A User's Guide to PRASSADCO)",** LPCE/NTS/073.D, Lab. Phys. Chimie Environ./CNRS, Orleans, France, 2003. (http://os.matfyz.cz/PRASSADCO/guide.pdf).

[9] K. Nykyri, B. Grison, P. J. Cargill, B. Lavraud, E. Lucek, I. Dandouras, A. Balogh, N. Cornilleau-Wehrlin, and H. Reme **Turbulence study in the highaltitude cusp: Cluster FGM and STAFF observations**, Ann Geophys., 24, 1057-1075, 2006.

[12] P. Robert, N. Cornilleau-Wehrlin, R. Piberne, Y. de Conchy, C. Lacombe, V. Bouzid, B. Grison, D. Alison, and P. Canu**: CLUSTER STAFF search coils magnetometer calibration – comparisons with FGM**, GID, 3, 679–751, 2013.

9. Appendix A: Coordinate systems used by STAFF

To transform telemetry data into significant physical units, we need to convert the data from the spinning system to a non-spinning one, with respect to Sun and Earth for instance. The following sections are dedicated to define all intermediate coordinate systems required for this operation. Notice than these definitions can be used for other experiments of the same type, on any other mission.
All transformation matrixes are named as: A_to_B where A and B are two different coordinate systems. To convert a vector given in the A system to the same vector expressed in the B system, the following expression is used:

$$\begin{pmatrix} x \\ y \\ y \end{pmatrix}_B = A\_to\_B \begin{pmatrix} x \\ y \\ y \end{pmatrix}_A$$

9.1 The Sensor Coordinate System (SCS)

This is the system where the original signal is measured (see Figure A below). It could be a non-perfect orthogonal system.

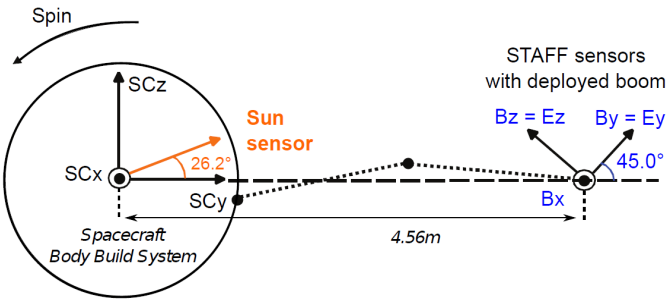

Figure A : The STAFF sensors in the spacecraft's system "SCS".

9.2 The Orthogonal Sensor System (OSS)

This is a Cartesian orthogonal coordinate system. Since, the original sensor system can be a non-orthogonal system, the first step is to transform the data vector into an orthogonal coordinate system: Z axis being the reference of the new Orthogonal Sensor System. The corresponding matrix, called "SCS_to_OSS", close to a unit matrix, is required and must be applied: values are supposed to be constant in time. Nevertheless, considering the low deviation of the sensor to an orthogonal system for CLUSTER/STAFF (~0.2°), this correction is not applied at this stage and the matrix is set to unity matrix.

$$SCS\_to\_OSS \cong \begin{pmatrix} 1 & 0 & 0 \\ 0 & 1 & 0 \\ 0 & 0 & 1 \end{pmatrix}$$

9.3 The Data Sensor System (DSS)

The Body Build System (BBS, see next section) is a system fixed to the geometry of the spacecraft, and is used as the spacecraft system reference for all the experiments. Generally, for most of spacecraft missions, the Z axis is close to the maximum principal inertia axis, also called the spin axis (for spin stabilized spacecraft). Nevertheless, for CLUSTER, this axis has been defined as the X axis.
However, in all our datasets, the convention taken is Z=spin axis. It means that we have an intermediate coordinate system, called Data Sensor System (DSS), which corresponds to the previous OSS, but where the axes are permuted, to make Z close to the spin axis.
With respect to Figure A, X_{OSS}, Y_{OSS}, Z_{OSS}, becomes Y, Z, X in DSS.
This permutation is obtained by the following matrix:

$$OSS\_to\_DSS = \begin{pmatrix} 0 & 1 & 0 \\ 0 & 0 & 1 \\ 1 & 0 & 0 \end{pmatrix}$$

9.4 The Body Build System (BBS)

In the case of CLUSTER, the Z axis of the Data Sensor System is close to the X axis of the BBS system, but the misalignment angle is not easy to determine. It is also true for the small angle between this X_{BBS} and the true spin axis (precession and nutation motions). Nevertheless, an estimate of the cumulative angle is done in next subsection. Here, we neglect this small misalignment and assume $Z_{DSS} = X_{BBS}$. In all cases, 2 other axis may be rotated by an important angle (see Figure A). The corresponding matrix is required, called "DSS_to_BBS": values are supposed to be constant. Practically, for the STAFF search coils of CLUSTER, this matrix is a rotation matrix of $\alpha = 45°$.

$$DSS\_to\_BBS = \begin{pmatrix} 0 & 0 & 1 \\ \cos\alpha & -\sin\alpha & 0 \\ \sin\alpha & \cos\alpha & 0 \end{pmatrix}$$

9.5 The Spin Reference System (SRS)

The spin reference system has its Z axis parallel to the spin axis. This is a spinning system, rotating at the spin frequency. As mentioned above, there is a small misalignment between the X_{BBS} axis and the Z_{SCS} axis, as there is another slight misalignment between the X_{BBS} axis and the Z_{DSS} axis (see Figure B).

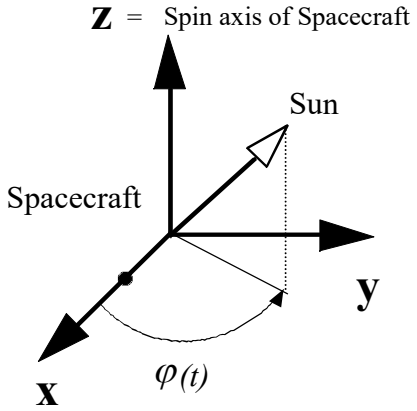

This is a spinning local system close to the measurement antenna of a spacecraft.

The Z-axis is the spin axis of the spacecraft.

The X-axis and Y-axis are perpendicular to the spin axis, and rotate at the spin frequency of the spacecraft.

The definition of the SR system requires knowledge of the spin axis in a fixed frame of reference (such as the GEI inertial system), and the value of the spin phase φ at a given time.

Figure B: Definition of the SR system

It is not easy to separate the two previous angles, but it is possible to estimate the small angle between the Z_{SCS} axis and the true spin axis which defines Z_{SRS}. This angle θ could be estimated by the measurement of the low spin signal on the Z_{SCS} component .
If B_{xs}, B_{ys}, B_{zs}, are the amplitudes in nT of the spin sine on the 3 x, y, z components of the SCS system, this angle is estimated by :

$$\sin\theta = \frac{B_{zs}\sqrt{2}}{\sqrt{B_{xs}^2 + B_{ys}^2 + B_{zs}^2}}$$

This angle could be constant, but can have also small variations during operations on the spacecraft (trajectory modifications, etc.). It has been estimated to an average value of ~0.5°, and has not been considered at this stage. So, the "BBS_to_SRS" matrix is a simple circular permutation set to:

$$BBS\_to\_SRS \cong \begin{pmatrix} 0 & 1 & 0 \\ 0 & 0 & 1 \\ 1 & 0 & 0 \end{pmatrix}$$

9.6 The spin reference2 system (SR2)

The SR2 system, also called "SSS" for Spacecraft-Sun System, or "DS" for despun, is derived from the SRS system by a *despin* operation. The spinning spacecraft is "stopped" just at the time where the X axis is in the plane containing the Z spin axis and the direction of the Sun. The rotation angle required is derived from the sun pulse or any other quantity to compute the spin phase angle φ_s (see Figure C).

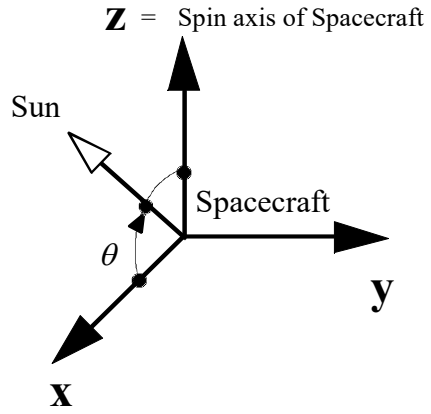

This is a fixed system useful for the spacecraft data processing. It is also called SSS, as "Spacecraft-Sun system", or DS system (Despun Spacecraft).

The Z-axis is the spin axis of the spacecraft.
The X-Z plane contains the direction of the Sun.

The X-axis is towards the day side.
The Y-axis is perpendicular to the spacecraft-Sun line.

The SR2 system rotates with the same period than the orbital period of the spacecraft with respect to the inertial system, while the declination θ varies continuously.

Figure C: Definition of the SR2 system (Despun)

This spin phase angle φ_s, and the corresponding time measurement, are required to build the "SRS_to_SR2" matrix. Terms of this matrix are fast-varying. The phase angle φ_s is calculated for each time tag of the data thanks to the sun pulse signal. With f_s as the spin frequency, we then have:

$$SRS\_to\_SR2 = \begin{pmatrix} \sin(2\pi f_s t + \varphi_s) & \cos(2\pi f_s t + \varphi_s) & 0 \\ \cos(2\pi f_s t + \varphi_s) & -\sin(2\pi f_s t + \varphi_s) & 0 \\ 0 & 0 & 1 \end{pmatrix}$$

9.7 The Inverse SR2 system (ISR2)

This is equivalent to the SR2 system (or SSS) where the Z and Y axis has inverse sign. This system is useful for CLUSTER, where the Z axis of ISR2 system is close to the Z axis of the GSE system, so ISR2 is a rather good approximation of the GSE system, and does not requires knowledge of spin direction in GSE system.

$$SR2\_to\_ISR2 = \begin{pmatrix} 1 & 0 & 0 \\ 0 & -1 & 0 \\ 0 & 0 & -1 \end{pmatrix}$$

9.8 Simplification of the cumulative matrix products

Cumulative matrix products requested to transform original data given in SCS coordinate to a fixed coordinate system such as SR2 can be strongly simplified if we neglect all small misalignment angles mentioned above. By the way, the first mass processing of the STAFF-SC data was a data base for the level 1 data (telemetry data) in the DSS system, which is delivered to the CSA. The only difference between the DSS with the SCS sensor coordinate is a circular permutation of the components to get the Z axis close to the spin axis, since we assume that the SCS is orthogonal and equal to the OSS.
So, to transform data expressed in DSS into the "fixed" SR2 we have to apply the cumulative matrix product:

$$\begin{pmatrix} x \\ y \\ y \end{pmatrix}_{SR2} = [SRS\_to\_SR2][BBS\_to\_SRS][DSS\_to\_BBS]\begin{pmatrix} x \\ y \\ y \end{pmatrix}_{DSS}$$

Assuming all small misalignment angles close to zero, we get:

$$[BBS\_to\_SRS][DSS\_to\_BBS] = \begin{pmatrix} \cos\alpha & -\sin\alpha & 1 \\ \sin\alpha & \cos\alpha & 0 \\ 0 & 0 & 0 \end{pmatrix}$$

Using expression of SRS_to_SR2 given in section 10.7, with $\omega_s = 2\pi f_s$ after some calculus we get:

$$\begin{pmatrix} x \\ y \\ z \end{pmatrix}_{SR2} = \begin{pmatrix} \sin(\omega_s t + \varphi_s + \alpha) & \cos(\omega_s t + \varphi_s + \alpha) & 1 \\ \cos(\omega_s t + \varphi_s + \alpha) & -\sin(\omega_s t + \varphi_s + \alpha) & 0 \\ 0 & 0 & 0 \end{pmatrix}\begin{pmatrix} x \\ y \\ z \end{pmatrix}_{DSS}$$

By neglecting all the small misalignment angles, the transformation from the Data Sensor System to the fixed SR2 system is simply reduced to a rotation in the spin plane of the fast-varying angle:

$$\psi = (\omega_s t + \varphi_s + \alpha).$$

This simplification is used for CLUSTER/STAFF calibration, but cannot be used for spacecraft or rocket having precession or nutation, or a non-constant direction of the spin axis. In this case, the full computation must be done.

9.9 The Geocentric Equatorial Inertial system (GEI)

The GSE system is a well-known system, with the Z axis perpendicular to the Ecliptic plane, and the X axis towards the Sun. To do the transformation from the SSS to the GSE, the direction of the spin axis in the GSE system is required. Due to the gyroscopic effect of a spinning spacecraft, the spin axis is ~constant in an inertial system, and so has a yearly variation in the GSE system, except during spacecraft operations (see Figure D).

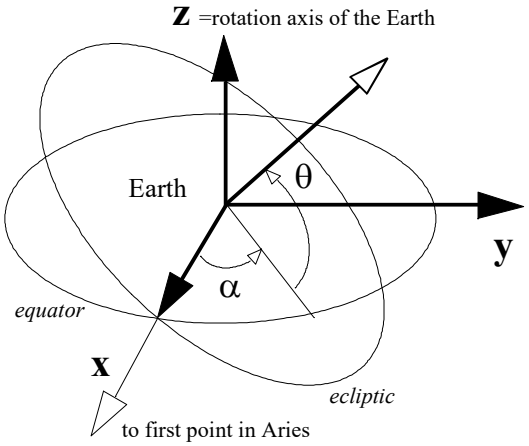

The Z-axis is parallel to the rotation axis of the Earth. The X-axis is defined by the intersection of the equator plane and the ecliptic plane, and is pointing towards the first point of Aries (Sun position at the vernal equinox). One can define the ***right ascension*** α *and the* ***declination*** θ *as:*

right ascension*:* $\alpha=\tan^{-1}(V_y/V_x)$

with α *in [0°,180°] for* $V_y>0$

α *in [180°,360°] for* $V_y<0$

declination $\theta=\sin^{-1}(V_z/V)$

with θ *in [-90°,90°]*

Figure D : Definition of the GEI system:

Note that in GSE system, each component mixes both parallel and perpendicular components to the spin axis. Because sensitivity is strongly different at low frequency on the parallel and perpendicular components in SR2 system, it is recommended to filter the data below ~0.6Hz before coordinate transformation. This is done for STAFF-SC Complex Spectra products delivered to the CSA.

9.10 The Geocentric Solar Ecliptic system (GSE)

Well known and often used system (see Figure E).

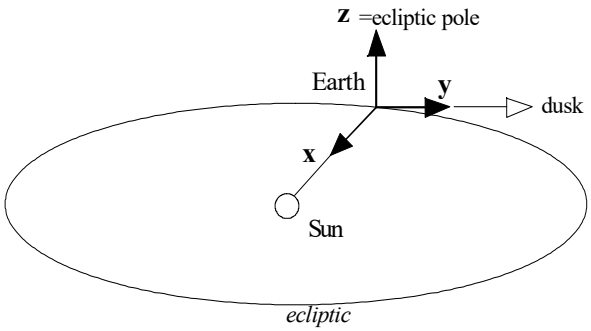

The X-axis is pointing from the Earth towards the Sun.

The X-axis and the Y-axis are included in the ecliptic plane.

The Y-axis is pointing toward the dusk, opposing to the planetary motion.

The Z-axis is parallel to the ecliptic pole. The GSE system has a yearly rotation with respect to the inertial system.

Figure E: Definition of the GSE system

9.11 Geocentric Solar Magnetospheric system (GSM)

This system is known in space physics to properly organize the data, insofar as it reconciles the direction of the Sun and the plane of the Earth magnetic meridian (see Figure F).

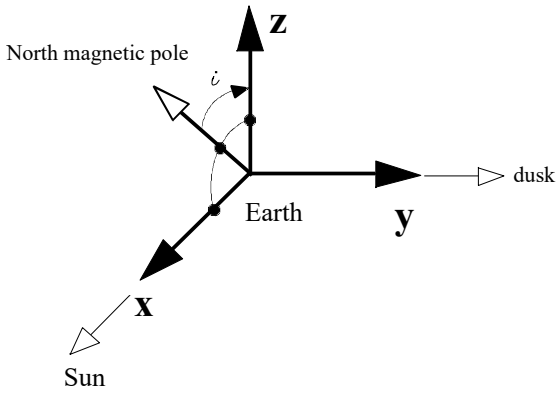

The X-axis is pointing from the Earth towards the Sun.

The X-Z plane contains the dipole axis.

The Y-axis is perpendicular to the Earth's magnetic dipole, towards the dusk and included in the magnetic equator plane.

Figure F6: Definition of the GSM system

The positive Z-axis is chosen to be in the same direction as the northern magnetic pole: the dipole tilt angle ***i*** is positive when the north magnetic pole is tilted towards the Sun. In addition to a yearly period due to the motion of the Earth about the Sun, the GSM system rotates the Solar direction with a 24 h period.

9.12 Magnetic Field Aligned system (MFA)

This system is essential to study the polarization of waves. Indeed, most of the plane waves are characterized by their direction of rotation around the magnetic field, and by the angle between the normal to the wave plane and the main field (see Figure G). It has therefore been introduced for this purpose.

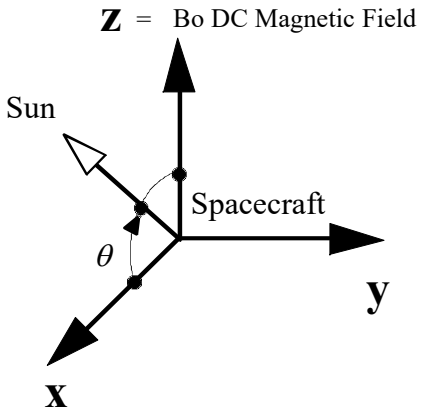

Figure G: Definition of the MFA system

This system is useful for physics, but the Bo DC magnetic field must be known, as well as its time variation
The Z-axis is the DC magnetic field vector.
The X-Z plane contains the direction of the Sun.

The X-axis is towards the day side.
The Y-axis is perpendicular to the spacecraft-Sun line.

The MFA system moves continuously with the time variation of the DC magnetic field.

10. Appendix B: In-Flight Calibration mode

STEP	SC command	Calibration Mode				Cal	Level	STAFF SA mode	STAFF SA mode
		Name	Signal	MWF	SA	Level		Low bit rate	High bit rate
1	0x011F	CAL4	White noise	Bx,By, Bz	E + B	1	0 dB	NM 2e	FM 3e
2	0x011F	CAL4	White noise	Bx,By, Bz	E + B	1	0 dB	NM 1	FM 2
3	0x011F	CAL4	White noise	Bx,By, Bz	E + B	1	0 dB	NM 2b	FM 3b
4	0x011F	CAL4	White noise	Bx,By, Bz	E + B	1	0 dB	NM 1	FM 1
5	0x013F	CAL4	White noise	Bx,By, Bz	E + B	2	-13 dB	NM 1	FM 1
6	0x015F	CAL4	White noise	Bx,By, Bz	E + B	3	-26 dB	NM 1	FM 1
7	0x017F	CAL4	White noise	Bx,By, Bz	E + B	4	-39 dB	NM 1	FM 1
8	0x019F	CAL4	White noise	Bx,By, Bz	E + B	5	-52 dB	NM 1	FM 1
9	0x01BF	CAL4	White noise	Bx,By, Bz	E + B	6	-65 dB	NM 1	FM 1
10	0x01DF	CAL4	White noise	Bx,By, Bz	E + B	7	-78 dB	NM 1	FM 1
11	0x01FF	CAL4	White noise	Bx,By, Bz	E + B	8	Gnd	NM 1	FM 1
12	0x011B	CAL3	White noise	Bx,By, Bz	E	1	0 dB	NM 1	FM 1
13	0x015B	CAL3	White noise	Bx,By, Bz	E	3	-26 dB	NM 1	FM 1
14	0x0113	CAL1	Sinus	Bx,By, REF		1	0 dB	NM 1	FM 1
15	0x0117	CAL2	Sinus	Bx,By, Bz		1	0 dB	NM 1	FM 1
16	0x0153	CAL1	Sinus	Bx,By, REF		3	-26 dB	EM	FM 1
17	0x0157	CAL2	Sinus	Bx,By, Bz		3	-26 dB	SM	FM 1
18	0x0193	CAL1	Sinus	Bx,By, REF		5	-52 dB	NM 1'e	FM 1
19	0x0197	CAL2	Sinus	Bx,By, Bz		5	-52 dB	NM 1'b	FM 1
20	0x01FF	CAL2	Sinus	Bx,By, Bz		8	Gnd	NM 1	FM 1
21	0x0103	CAL OFF redundant	--	Bx,By, Bz		1	BKG	NM 1	FM 1
22	0x0157	CAL2	Sinus	Bx,By, Bz		3	-26 dB	NM 1	FM 1
23	0x0100	CAL Off/	--	Bx,By, Bz		1	BKG	NM 1	FM 1

Parameters of each of the 23 steps in an in-flight calibration sequence in NBR and HBR telemetry. The occurrence of each step is provided in STAFF Status Word#1 (see Users Guide).

```
;PROCESSING DATE: Tue Feb  5 14:23:58 2013
;CALIBRATION CARACTERISTICS ARE
;      SPACECRAFT NUMBER: 2
;      EXPERIMENT       : STAFF SC
;      TELEMETRY CADENCE: NORMAL BIT RATE
;CALIBRATION DATE: 2007-05-04 05:12:12
;

 Step   Band (Hz)    Bx (Vr)     By (Vr)     Bz (Vr)
*****************************************************
1 - 4     1  - 3      4.55e-04    5.09e-03    5.85e-03
          3  - 6      1.08e-03    2.24e-03    2.42e-03
          6  - 9      1.76e-03    2.09e-03    2.31e-03
          9  - 11     1.65e-03    2.02e-03    2.01e-03
          11 - 12.5   1.01e-03    1.47e-03    1.36e-03

 Band :  7 - 9  Hz
 Step    Bx (Vr)     By (Vr)     Bz (Vr)
****************************************
 12       1.90e-03    1.98e-03    2.40e-03
 13       1.04e-04    1.50e-03    1.29e-03

 Frequency : 7.20 Hz
 Step    Bx (Vr)     By (Vr)     Bz (Vr)     Ph. Bx/Bz    Ph. By/Bz
*************************************************************************
 14       1.95e-01    1.93e-01    1.26e+00    242.3        242.1
 15       1.94e-01    1.93e-01    1.86e-01    358.6        359.0
 16       9.76e-03    9.96e-03    6.35e-02    242.7        229.6
 17       9.77e-03    7.44e-03    8.06e-03    360.0        354.6
 18       4.82e-04    3.72e-04    3.19e-03    248.7        203.3
 19       4.60e-04    2.24e-03    1.55e-03    326.1        192.7
 22       9.66e-03    7.11e-03    1.03e-02    358.7          2.7

 Band :  6 - 9  Hz
 Step    Bx (Vr)     By (Vr)     Bz (Vr)
****************************************
 20       1.31e-03    5.79e-02    3.52e-02
 21       1.54e-03    4.22e-03    6.68e-02

 Step   Band (Hz)    Bx (Vr)     By (Vr)     Bz (Vr)
*****************************************************
 23       0  - 3      1.55e-02    1.20e+00    1.20e+00
          3  - 6      2.09e-03    8.30e-02    6.58e-02
          6  - 9      1.57e-03    5.28e-02    4.16e-02
          9  - 12.5   1.24e-03    4.92e-02    3.81e-02
STEP 1 TO 4
BAND 1.0 - 3.0  ANOMALY ON BX  4.55e-04   REF = 3.00e-04   DEVIATION  51.67 %
```

Example of the routine report for each calibration sequence

The report delivered for each calibration sequence of the SC instruments lists:

- A general information of this sequence (date, spacecraft number)
- The values obtained for some steps after averaging of the computed spectra and for each component (amplitude and phase)

For each step except 14-22, there are 400 samples in NBR (1800 HBR) from which the 200 in the middle of the step are considered to produce a spectrum with a 0.14648 frequency resolution. Then the Vrms amplitude is averaged over the frequency band indicated for each step. For the range 0-3 Hz of Step 1-4 the first 2 frequency bins, close to the spin frequency are eliminated.

For step 14-22 where a sine wave is used, the strongest peak in the range 6.7 to 7.6 Hz is searched for by step of 0.1 Hz and its amplitude and phase ratio is used in the report.
The process is the same in HBR, with different bandwidth (0-50 Hz, 50-105 Hz, 105-160 Hz, 160 -200 Hz, 200-225 Hz) and a sine wave stimulus at 101 Hz.
A reference value for each of these steps has been provided from ground-based calibration.
For each step, when these values exceed by more than 50% the reference value, an alarm is generated and an "Anomaly" warning line appears at the bottom of the report. The line shows the observed value on the step, its reference value and the exceedance of this reference (in %). Calibration sequences for which the telemetry stream does not allow a complete report to be generated have not been archived.

Users should keep in mind that the reference values were obtained without external source of perturbation. In flight, when an anomaly line is triggered by a strong natural signal significantly exceeding the reference, the calibration sequence has no meaning. The level of natural emissions seen by the instrument is provided by Step 23.